

THE UNIVERSITY OF MICHIGAN
INDUSTRY PROGRAM OF THE COLLEGE OF ENGINEERING

LARGE-AMPLITUDE MOTION OF A COMPRESSIBLE
FLUID IN THE ATMOSPHERE

Alfons J. Claus

A dissertation submitted in partial fulfillment
of the requirements for the degree of
Doctor of Philosophy in The
University of Michigan
Department of Engineering Mechanics
1961

June, 1961

IP-521

engr

UMR1229

Doctoral Committee:

Professor Chia-Shun Yih, Chairman
Assistant Professor William P. Graebel
Professor Jesse Ormondroyd
Professor Earl D. Rainville
Professor Mahinder S. Uberoi

ACKNOWLEDGMENTS

The author wishes to express his appreciation to Professor Chia-Shun Yih, chairman of the committee who suggested the topic and under whose direction the work was performed. Thanks are due to the committee members for their efforts and interest.

The research was partially supported by the Army Research Office (Durham) through a contract with the University of Michigan. The author received a predoctoral fellowship granted by the Institute of Science and Technology.

The work would have been impossible without the use of the facilities of the computing center of the University of Michigan.

The aid of the Industry Program of the College of Engineering in the final preparation of the manuscript is much appreciated.

TABLE OF CONTENTS

	<u>Page</u>
ACKNOWLEDGMENTS.....	ii
LIST OF FIGURES.....	iv
NOMENCLATURE.....	vi
I. INTRODUCTION.....	1
II. THE GOVERNING DIFFERENTIAL SYSTEM.....	3
III. UPSTREAM CONDITIONS LEADING TO A LINEAR DIFFERENTIAL EQUATION.....	10
IV. METHODS OF SOLUTION.....	16
V. DISCUSSION OF RESULTS.....	28
VI. COMPARISON WITH FLOW OF AN INCOMPRESSIBLE FLUID.....	40
VII. CONCLUSIONS.....	54
APPENDIX I. INTEGRATION OF EQUATION (21).....	56
APPENDIX II. CALCULATION OF THE EIGENVALUES AND EIGENFUNCTIONS..	59
APPENDIX III. CALCULATION OF THE FUNCTIONS $F_0(z)$ AND $F_1(z)$	65
APPENDIX IV. TABLES I THROUGH XVIII.....	68
BIBLIOGRAPHY.....	74

LIST OF FIGURES

<u>Figure</u>		<u>Page</u>
1	Mathematical Model for the Study of Two Dimensional Flows in the Troposphere.....	9
2	Upstream Conditions Leading to a Linear Differential System.....	15
3	Flow Regions in Long's Method.....	22
4	Upstream Conditions Leading to a Flow Pattern With No Leewave Components.....	22
5	Flow Pattern With No Leewaves.....	30
6	Upstream Conditions Leading to a Flow Pattern With One Leewave Component.....	31
7	Flow Pattern With One Leewave Component.....	32
8	Influence of Wind Profile on Wave Amplitude.....	33
9	Isothermal Lines in the Flow With One Leewave Component.....	34
10	Upstream Conditions Leading to a Flow Pattern With Two Leewave Components.....	35
11	Flow Pattern With Two Leewave Components.....	38
12	Upstream Conditions for an Incompressible Fluid and Leading to Equation (71).....	42
13	Upstream Conditions Used for the Comparison Between the Flow of an Incompressible Fluid and the Flow of a Compressible Fluid.....	44
14	Stratification of Density, Pressure, Temperature and Entropy in the Atmosphere and Illustrating the Concept of Potential Density.....	44
15	Relocation of a Particle in a Quiescent Atmosphere Illustrating the Concept of Potential Density.....	44
16	Approximation of the Stratification of Potential Density in a Compressible Fluid by the Density Stratification in an Incompressible Fluid. Both Stratifications Lead to Linear Governing Equations.....	49

LIST OF FIGURES (CONT'D)

<u>Figure</u>		<u>Page</u>
17	Comparison Between the Flow of an Incompressible and a Compressible Fluid. Incompressible Case.....	51
18	Comparison Between the Flow of an Incompressible and a Compressible Fluid. Compressible Case.....	52
19	Iterative Scheme for the Calculation of the Eigenvalues of the Sturm-Liouville System Consisting of (31) and (32).....	62

NOMENCLATURE

Dimensional Form	Dimensionless Form	
P_*	p	pressure
ρ_*	ρ	density
T_*	T	temperature
S_*	S	entropy
x_1, x_3	x, z	rectangular Cartesian coordinates; (x_3, z) upward
u_1, u_3	u, w	velocity components
u'_1, u'_3	u', w'	components of associated velocity
	U	velocity far upstream
	U'	associated velocity far upstream
q'_*	q'	associated speed
η'_*	η'	vorticity of associated velocity field
ρ'_*	ρ'	associated density
ψ'_*	ψ'	associated stream function
	ψ'_1	associated nonhomogeneous stream function
	ψ'_2	associated homogeneous stream function
H_*	H'	specific energy corresponding to associated flow
P_0, ρ_0, T_0, S_0		pressure, density, temperature and entropy respectively at the reference point $z = 0.5$ (far upstream)
d		height of the tropopause
g		gravitational acceleration
	λ	potential density
	γ	<u>specific heat by constant pressure</u> <u>specific heat by constant volume</u>
∇_*^2	∇^2	Laplacian operator

I. INTRODUCTION

Large-amplitude atmospheric flows past mountain ridges are investigated. The flows are assumed to be steady and two-dimensional. Since diffusive and viscous effects are of minor importance in most atmospheric phenomena, they are neglected. The compressibility of the air is taken into account. However, effects of dynamic compressibility will be ignored because the Mach number can be assumed everywhere small. This is equivalent to assuming that any change in density of a particle* is entirely due to a change in its elevation.

The larger part of this investigation is devoted to the study of waves in the lee of mountain ridges. The presence of these waves is essentially a result of the non-homentropy and non-homenergy of the atmosphere. However, the analysis of non-homentropic flows is greatly complicated by the lack of a unique relationship between pressure and density, valid throughout the whole field of flow. Several authors (Lyra, Queney, Scorer, Crapper) have studied the subject by perturbation methods. Therefore, their results are valid only when the disturbances are small compared with the corresponding quantities in the undisturbed flow. The major contribution of the present investigation consists in the treatment of the large amplitude motion. In the study to be presented here, the flows are governed by an equation whose form depends on the conditions far upstream of the mountain ridge. Some of these conditions make the latter equation

* By a particle is meant a small volume of air.

linear provided stratifications of entropy and specific energy are slight, and the Mach number is indeed everywhere small as assumed. These particular upstream conditions thus give rise to large amplitude flows which are still governed by a linear equation.

The linearity of the equation imposes some restrictions on wind profile and stratification of the relevant physical quantities far upstream of the ridge. However, the method has proven to be quite flexible and several flow patterns have been obtained corresponding to various upstream conditions which are realistic.

In order to investigate the effect of compressibility, two flow patterns with equivalent upstream conditions, one for a compressible fluid and the other for an incompressible fluid, were obtained and compared with each other. A discussion of equivalent upstream conditions is included.

II. THE GOVERNING DIFFERENTIAL SYSTEM

The equations of motion for steady two-dimensional flows of an inviscid fluid are

$$u_1 \frac{\partial u_1}{\partial x_1} + u_3 \frac{\partial u_1}{\partial x_3} = - \frac{1}{\rho_*} \frac{\partial p_*}{\partial x_1} , \quad (1a)$$

and

$$u_1 \frac{\partial u_3}{\partial x_1} + u_3 \frac{\partial u_3}{\partial x_3} = - \frac{1}{\rho_*} \frac{\partial p_*}{\partial x_3} - g . \quad (1b)$$

The equation of continuity is

$$\frac{\partial(\rho_* u_1)}{\partial x_1} + \frac{\partial(\rho_* u_3)}{\partial x_3} = 0 . \quad (2)$$

If diffusive effects are neglected the quantity p_*/ρ_*^γ is constant along a pathline and, for steady flows, also constant along a streamline. However, for the flow of a non-homentropic fluid considered here, the value of p_*/ρ_*^γ changes from streamline to streamline. Therefore ρ_* is not a function of p_* alone throughout the whole field of flow, and the expression dp_*/ρ_* is not a total differential. This major difficulty can be avoided by introducing an associated flowfield which is related to the old one by means of a transformation due to Yih (1960):

$$u_1' = u_1 \sqrt{\lambda} , \quad u_3' = u_3 \sqrt{\lambda} , \quad \rho_*' = \frac{\rho_*}{\lambda} , \quad p_*' = p_* ,$$

with

$$\lambda = \frac{\rho_*}{\rho_0} \left(\frac{p_0}{p_*} \right)^{1/\gamma} .$$

When the above changes of dependent variables are utilized, Equations (1a) and (1b) become

$$u_1^i \frac{\partial u_1^i}{\partial x_1} + u_3^i \frac{\partial u_1^i}{\partial x_3} = - \frac{1}{\rho_*^i} \frac{\partial p_*^i}{\partial x_1} \quad (3a)$$

and

$$u_1^i \frac{\partial u_3^i}{\partial x_1} + u_3^i \frac{\partial u_3^i}{\partial x_3} = - \frac{1}{\rho_*^i} \frac{\partial p_*^i}{\partial x_3} - g\lambda, \quad (3b)$$

in which ρ_*^i now depends solely on p_*^i . Indeed

$$\rho_*^i = \frac{\rho_*}{\lambda} = \frac{\rho_*}{\frac{\rho_*}{\rho_0} \left(\frac{p_0}{p_*}\right)^{1/\gamma}} = \rho_0 \left(\frac{p_*^i}{p_0}\right)^{1/\gamma}. \quad (4)$$

The equation of continuity becomes

$$\frac{\partial(\rho_*^i u_1^i)}{\partial x_1} + \frac{\partial(\rho_*^i u_3^i)}{\partial x_3} = 0. \quad (5)$$

Equation (5) guarantees the existence of a stream function $\psi_*^i(x_1, x_3)$, in terms of which the velocity components can be expressed as

$$u_1^i = \frac{\rho_0}{\rho_*^i} \frac{\partial \psi_*^i}{\partial x_3}, \quad u_3^i = - \frac{\rho_0}{\rho_*^i} \frac{\partial \psi_*^i}{\partial x_1}. \quad (6)$$

With $\eta_*^i = \frac{\partial u_1^i}{\partial x_3} - \frac{\partial u_3^i}{\partial x_1}$, Equations (3a) and (3b) can be written as

$$u_3^i \eta_*^i = - \frac{1}{\rho_*^i} \frac{\partial p_*^i}{\partial x_1} - \frac{\partial}{\partial x_1} \left(\frac{q_*^{i2}}{2} \right) \quad (7a)$$

and

$$- u_1^i \eta_*^i = - \frac{1}{\rho_*^i} \frac{\partial p_*^i}{\partial x_3} - \frac{\partial}{\partial x_3} \left(\frac{q_*^{i2}}{2} \right) - g\lambda, \quad (7b)$$

or, by virtue of Equations (6),

$$\frac{\rho_0}{\rho_*^i} \eta_*^i \frac{\partial \psi_*^i}{\partial x_1} = \frac{\partial I^i}{\partial x_1} \quad (8)$$

and

$$\frac{\rho_0}{\rho_*^i} \eta_*^i \frac{\partial \psi_*^i}{\partial x_3} = \frac{\partial I^i}{\partial x_3} + g\lambda, \quad (9)$$

in which

$$I^i = \frac{\gamma p_0}{(\gamma-1)\rho_0} \left(\frac{p_*^i}{p_0}\right)^{\gamma-1/\gamma} + \frac{q_*^{i2}}{2}$$

Multiplication of Equation (8) by dx_1 and (9) by dx_3 , and addition of the results produce

$$\frac{\rho_0}{\rho_*^i} \eta_*^i d\psi_*^i = dI^i + g\lambda dx_3 = dH_*^i - g x_3 d\lambda, \quad (10)$$

where H_*^i is now

$$H_*^i = \frac{\gamma p_0}{(\gamma-1)\rho_0} \left(\frac{p_*^i}{p_0}\right)^{\gamma-1/\gamma} + \frac{q_*^{i2}}{2} + g\lambda x_3 \quad (11)$$

But λ and H_*^i are functions of ψ_*^i alone. ** Thus

$$\frac{\rho_0}{\rho_*^i} \eta_*^i + g x_3 \frac{d\lambda}{d\psi_*^i} = \frac{dH_*^i}{d\psi_*^i} \quad (12)$$

Finally, with (6), Equation (12) can be written as

$$\nabla_*^2 \psi_*^i - \frac{1}{\rho_*^i} \left(\frac{\partial \rho_*^i}{\partial x_1} \frac{\partial \psi_*^i}{\partial x_1} + \frac{\partial \rho_*^i}{\partial x_3} \frac{\partial \psi_*^i}{\partial x_3} \right) + g x_3 \frac{\rho_*^{i2}}{\rho_0^2} \frac{d\lambda}{d\psi_*^i} = \frac{\rho_*^{i2}}{\rho_0^2} \frac{dH_*^i}{d\psi_*^i} \quad (13)$$

** The fact that H_*^i is constant along a streamline can easily be verified by showing that $DH_*^i/Dt = 0$.

Aside from the stream function ψ'_* , the density ρ'_* is another unknown appearing in (13). However ρ'_* can be expressed in terms of ψ'_* by means of Equation (11). As far as this evaluation is concerned, it is clear that if the term $q'^2_*/2$ in (11) is maintained, the resulting equation for ψ'_* would be extremely complicated. We will therefore neglect the term $q'^2_*/2$ in the evaluation of ρ'_* . This measure is equivalent to assuming that the change of density is solely due to a change in elevation, i.e., that the dynamic compressibility is negligible or the Mach number is small, which is certainly true for most atmospheric phenomena.

Furthermore, we will only consider flows for which the variation of H'_* and λ is small enough for the assumption of their constancy in (11) to be justified. This is not in contradiction to the fact that the terms containing $d\lambda/d\psi'_*$ and $dH'_*/d\psi'_*$ in (13) are maintained. It is indeed possible for the quantities $d\lambda/d\psi'_*$ and $dH'_*/d\psi'_*$ to be of the order of magnitude as the remaining terms in (13) and still be such that the variations of λ and H'_* are small in the whole field of flow. For a more complete discussion of above assumptions we refer to [13]. Taking H'_* and λ as constants ($\lambda = 1$) and neglecting $q'^2_*/2$, the density can be evaluated by

$$\left(\frac{\rho'_*}{\rho_0}\right)^{\gamma-1} = \frac{H'_* - gx_3}{K}, \quad (14)$$

in which

$$K = \frac{\gamma P_0}{(\gamma-1)\rho_0}$$

Combination of (13) with (14) produces

$$\begin{aligned} \nabla_*^2 \psi_*' + \frac{1}{\gamma-1} \cdot \frac{g}{H_*' - gx_3} \frac{\partial \psi_3'}{\partial x_3} + gx_3 \left(\frac{H_*' - gx_3}{K} \right)^{2/\gamma-1} \frac{d\lambda}{d\psi_*'} \\ = \left(\frac{H_*' - gx_3}{K} \right)^{2/\gamma-1} \frac{dH_*'}{d\psi_*'} \end{aligned} \quad (15)$$

The functions $\lambda(\psi_*')$ and $H_*'(\psi_*')$ are to be considered as known and are conveniently determined far upstream. (See Section 3).

Equation (15) will be used for the study of two-dimensional, atmospheric flows past mountain ridges. Except for the obstacle (mountain profile), the ground will be considered perfectly level which implies that the stream function $\psi_*'(x_1, x_3)$ on the level portion of the ground is equal to a constant and can be taken equal to zero.

The fact that there is no rigid upper boundary for the atmosphere causes some difficulty. However, due to the very stable stratification (constant temperature) in the stratosphere, vertical motion in that layer is somewhat inhibited. If we assume no vertical displacement in the stratosphere, the interface between the troposphere and stratosphere may be considered to be a rigid plane. The flows studied under this assumption are therefore flows in the troposphere. If d is the height of this interface (tropopause), the above assumption is mathematically equivalent to $\psi_*'(x_1, d) = \text{constant}$, which is a second boundary condition for $\psi_*'(x_1, x_3)$. With the dimensionless variables

$$\begin{aligned} x &= \frac{x_1}{d}, \quad z = \frac{x_3}{d}, \quad \psi' = \frac{\psi_*'}{d\sqrt{gd}}, \quad H' = \frac{1}{\alpha} = \frac{H_*'}{gd}, \\ \beta &= \left(\frac{\gamma-1}{\gamma} \right)^{2/\gamma-1} \left(\frac{\rho_0 H_*'}{p_0} \right)^{2/\gamma-1}, \quad (u, w) = \frac{(u_1, u_3)}{\sqrt{gd}}, \end{aligned}$$

Equation (15) can be put in the form

$$\begin{aligned} \nabla^2 \psi' + \frac{1}{\gamma-1} \frac{\alpha}{1-\alpha z} \frac{\partial \psi'}{\partial z} + \beta z (1-\alpha z)^{2/\gamma-1} \frac{d\lambda}{d\psi'} \\ = \beta (1-\alpha z)^{2/\gamma-1} \frac{dH'}{d\psi'} \end{aligned} \quad (16)$$

The boundary conditions become

$$\psi'(x,0) = 0 \quad (17a)$$

for values of x corresponding to the level portion of the ground, and

$$\psi'(x,1) = \text{constant} \quad (17b)$$

The atmosphere has thus been replaced by a mathematical model (See Figure 1) in which the essential physical features have been retained and should be quite adequate for the study of atmospheric flows over mountain ridges. This mathematical model consists of a channel bounded by two rigid horizontal planes located at $z = 0$ and $z = 1$ in a rectangular cartesian coordinate system. An obstacle is present on the lower boundary. The flow is governed by the system consisting of Equations (16) and (17). The form of Equation (16) depends on the upstream conditions since they determine the functions $d\lambda/d\psi'$ and $dH'/d\psi'$. These conditions will be discussed in some detail in the next section.

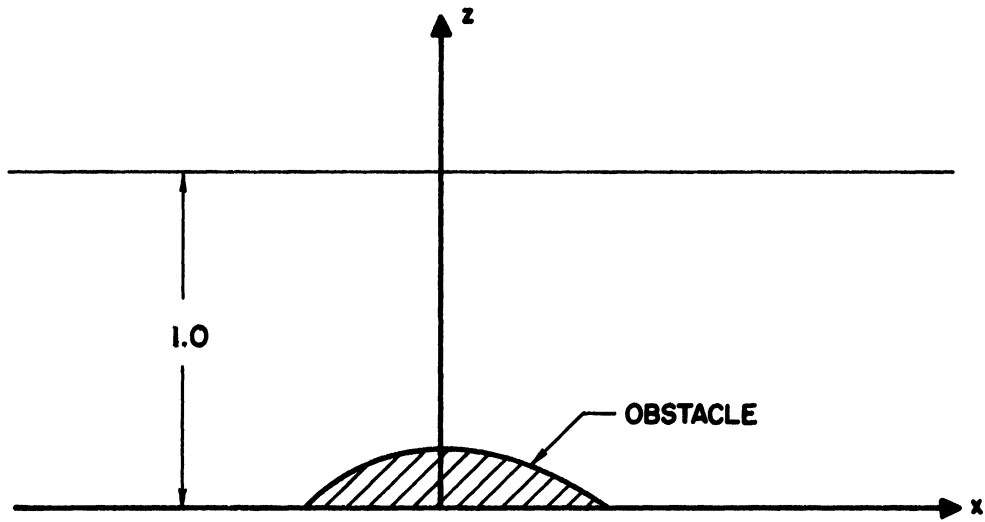


Figure 1. Mathematical Model for the Study of Two Dimensional Flows in the Troposphere.

III. UPSTREAM CONDITIONS LEADING TO A LINEAR DIFFERENTIAL EQUATION

In order to have a clear physical picture of what is meant by conditions upstream, a uniform flow between the two rigid planes ($z = 0$ and $z = 1$) with no obstacle present can be considered. It is obvious that the pressure, density, temperature and velocity profiles do not depend on the section at which they are taken. Suppose that, at a certain time, an obstacle is introduced. If the resulting unsteady flow tends to a steady state and furthermore if the introduction of the obstacle does not alter the distributions of p , ρ , T , and U sufficiently far upstream, the conditions far upstream can be considered as pre-assigned.

First of all let it be observed that, out of the four functions, $p(z)$, $\rho(z)$, $T(z)$, $U(z)$, only two can be chosen arbitrarily, namely the velocity $U(z)$ and any one of $p(z)$, $\rho(z)$, and $T(z)$, say $\rho(z)$. Indeed, since far upstream the flow is uniform, the pressure p can be obtained from ρ by means of the equation $\frac{dp}{dz} = -\frac{g\rho_0 d}{p_0} \rho$. The temperature T follows then from the gas law.

If the velocity and density are given (as functions of z) far upstream, all the four quantities p , ρ , T , and U are known and λ can be determined from $\lambda = \rho p^{-1/\gamma}$. The specific energy H' can then be evaluated using the relation

$$H' = E p^{\gamma-1/\gamma} + \frac{\lambda U^2}{2} + \lambda z, \quad (18)$$

in which

$$E = \frac{\gamma p_0}{(\gamma-1)\rho_0 g d}.$$

Furthermore, far upstream, $U' = U\sqrt{\lambda}$ and ψ' are related by

$$U' = \frac{1}{\rho'} \frac{d\psi'}{dz} = \frac{\lambda}{\rho} \frac{d\psi'}{dz} \quad \text{or} \quad U = \frac{\sqrt{\lambda}}{\rho} \frac{d\psi'}{dz} ,$$

or else

$$\psi' = \int_0^z \frac{\rho U}{\sqrt{\lambda}} dz .$$

We have thus H' , λ and ψ' as functions of z far upstream and H' and λ can be determined as functions of ψ' . The latter functional relationships are valid throughout the whole field of flow and, as pointed out earlier, they determine the form of the governing differential equation.

In the search for a solvable system we will try to obtain linear functions of ψ' for $d\lambda/d\psi'$ and $dH'/d\psi'$. Clearly, a random choice of the upstream density ρ and velocity U would, in general, not lead to a linear dependence of $dH'/d\psi'$ and $d\lambda/d\psi'$ on ψ' . The adopted scheme will therefore be an inverse one. Since we have the choice of two arbitrary functions (for instance U and ρ) of z , we shall so choose them as to insure the linear dependence of $dH'/d\psi'$ and $d\lambda/d\psi'$ on ψ' . Thus, we put

$$\frac{d\lambda}{d\psi'} = A\psi' + B \tag{19a}$$

and

$$\frac{dH'}{d\psi'} = C\psi' + D . \tag{19b}$$

Once the constants A, B, C, D are chosen, it is possible to determine the upstream situation. That this is indeed so can be best shown by determining the upstream condition corresponding to a certain choice of A, B, C, D which will now be done.

Inserting the Expressions (19) for $d\lambda/d\psi'$ and $dH'/d\psi'$ into Equation (16), we obtain:

$$\begin{aligned} \nabla^2 \psi' + \frac{1}{\gamma-1} \frac{\alpha}{1-\alpha z} \frac{\partial \psi'}{\partial z} + \beta(1-\alpha z)^{\frac{2}{\gamma-1}} (Az-C)\psi' \\ = \beta(1-\alpha z)^{\frac{2}{\gamma-1}} (D-Bz) . \end{aligned} \quad (20)$$

Since the flow far upstream is essentially uniform, the stream function becomes a function of z alone, say $\psi'_1(z)$, and is governed by

$$\begin{aligned} \frac{d^2 \psi'_1}{dz^2} + \frac{1}{\gamma-1} \frac{\alpha}{1-\alpha z} \frac{d\psi'_1}{dz} + \beta(1-\alpha z)^{\frac{2}{\gamma-1}} (Az-C)\psi'_1 \\ = \beta(1-\alpha z)^{\frac{2}{\gamma-1}} (D-Bz) , \end{aligned} \quad (21)$$

which is an ordinary differential equation for $\psi'_1(z)$. Any function $\psi'_1(z)$ satisfying (21) guarantees the linearity of (16). The actual integration is done in Appendix I. Once $\psi'_1(z)$ is known, λ and H' as functions of z (far upstream) are easily determined. Indeed it follows from (19a) and (19b) that

$$\lambda = \frac{A\psi'_1{}^2}{2} + B\psi'_1 + \lambda_0 , \quad (22a)$$

and

$$H' = \frac{C\psi'_1{}^2}{2} + D\psi'_1 + H'_0 . \quad (22b)$$

The constant λ_0 can be chosen to make $\lambda = 1$ at the reference point, i.e., the point where the pressure and density are p_0 and ρ_0 respectively. This point has been taken at $z = 0.5$ in our calculations. The constant H'_0 has to be taken in such a way as to make $\alpha \approx 1/H'$. Since one of the earlier assumptions was that the variation in H' is small, $\alpha = 1/H'$

was treated as a constant in Equation (21). By selecting H'_0 as indicated, H' (slightly varying with height) will be consistent with the value of α appearing in (21).

It follows from (18) that

$$p = \left[\frac{H' - \lambda z - \frac{U'^2}{2}}{E} \right]^{\frac{\gamma}{\gamma-1}} \quad (23)$$

Furthermore

$$U' = p^{-1/\gamma} \frac{d\psi'_1}{dz} \quad (24)$$

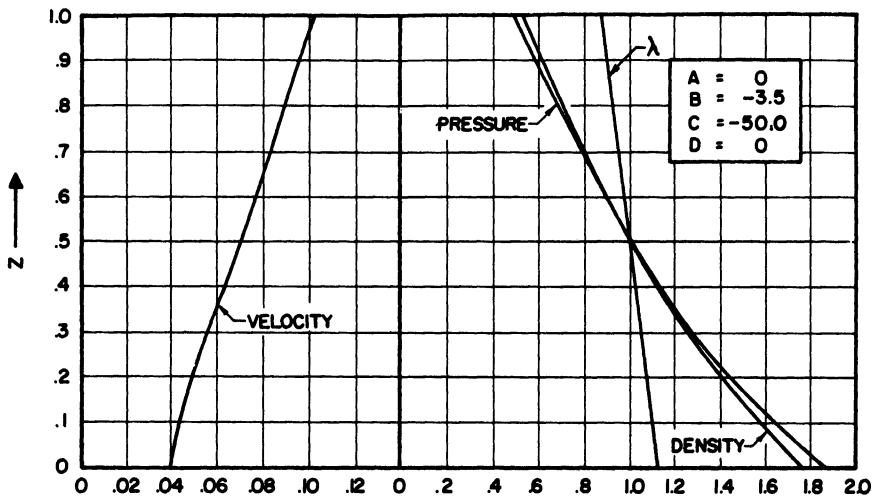
The only unknowns appearing in Equations (23) and (24) are p and U' . Since U'^2 is usually very small with respect to the other terms in (23), the system can best be solved using an iterative scheme. To find p and U' for a certain value of z , λ and H' are computed from (22). With $U' = 0$, Equation (23) gives an approximate value for p which, in turn, can be put into (24) to yield a first approximation for U' . This latter value of U' can now be used to get, by means of Equation (23), a more accurate value of p , etc. The procedure can be stopped when two successive values of p (or U') are sufficiently close together. Once U' and p are known the velocity U and density ρ follow then from $U = U'/\sqrt{\lambda}$ and $\rho = \lambda p^{1/\gamma}$.

The previously obtained pressure $p(z)$ and density $\rho(z)$ satisfy the equation of static equilibrium $\frac{dp}{dz} = -\frac{g\rho_0 d}{p_0} \rho$. This is indeed guaranteed by the fact that Equation (21) is the equation of static equilibrium in terms of the stream function $\psi'_1(z)$.

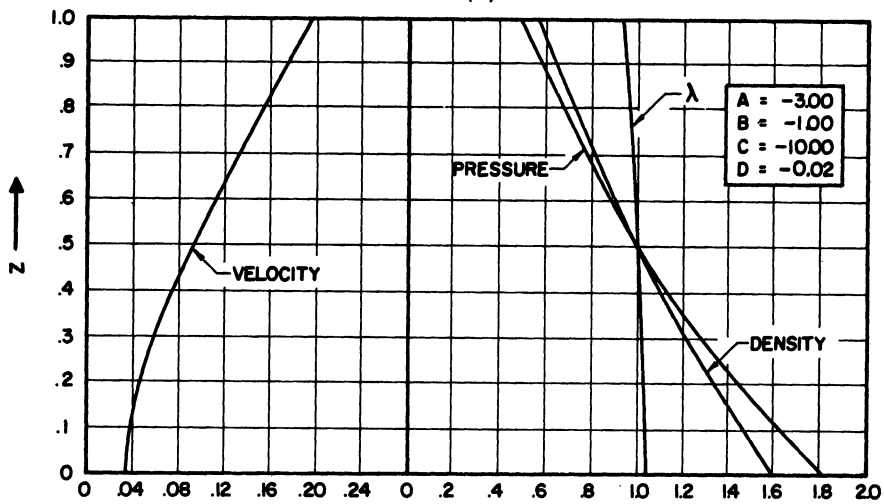
Since Equation (21) does not uniquely determine $\psi'_1(z)$, the same set of values of A , B , C , and D corresponds to different upstream conditions

and therefore leaves this inverse procedure quite flexible. It may therefore be hoped that a realistic upstream situation can be found, first by selecting proper values for A, B, C, and D and further, once a definite choice has been made, by taking the most suitable solution of (21).

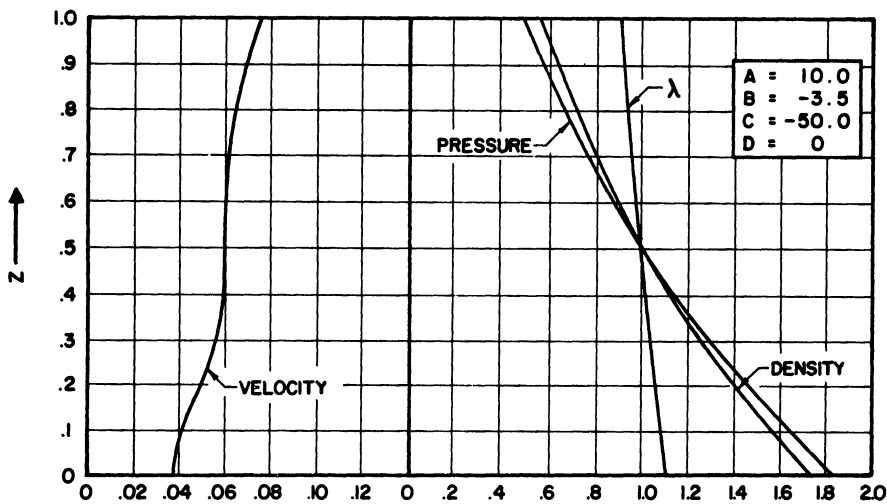
Equation (21) has been solved by a series method. Various realistic upstream conditions have been obtained. Some of them are shown in Figure 2. In all cases the density stratification fits meteorological data very closely. This density stratification is quite independent of the values of A, B, C, and D as long as the velocity is kept within reasonable limits. Furthermore these coefficients by no means determine the stratification in entropy and specific energy, but merely establish some relationship between this stratification and the velocity. Roughly an increase in the velocity leads, for constant A, B, C, and D, to a greater stratification. Entropy-stratification and wind profiles actually occurring in the atmosphere can be approximated quite closely as can be seen from Figure 2. The present analysis is therefore not without practical value.



(a)



(b)



(c)

Figure 2. Upstream Conditions Leading to a Linear Differential System.

IV. METHODS OF SOLUTION

The basic problem can now be stated more accurately. Suitable values have been assigned to the constants A, B, C, and D, and, out of the infinity of solutions of (21), an appropriate stream function $\psi_1'(z)$ has been selected corresponding to realistic upstream conditions. The problem is then to find a function $\psi'(x,z)$ satisfying Equation (20), which is equal to zero on the lower boundary (consisting of the level portion $z = 0$ and the obstacle) and equal to $\psi_1'(1)$ on the upper boundary $z = 1$. Furthermore $\psi'(x,z)$ should approach $\psi_1'(z)$ for $x \rightarrow -\infty$. Thus, if we put

$$\psi'(x,z) = \psi_1'(z) + \mu \psi_2'(x,z) \quad (25)$$

into (20), the function $\psi_2'(x,z)$ has to satisfy the homogeneous Equation (26), since $\psi_1'(z)$ is a solution of (21). Thus,

$$\nabla^2 \psi_2' + \frac{1}{\gamma-1} \frac{\alpha}{1-\alpha z} \frac{\partial \psi_2'}{\partial z} + \beta(1-\alpha z)^{2/\gamma-1} (Az-C) \psi_2' = 0 \quad (26)$$

Furthermore $\psi_2'(x,z)$ is subject to the conditions:

$$1) \quad \psi_2'(x,z) = 0 \quad \text{on the lower boundary,} \quad (27)$$

$$2) \quad \psi_2'(x,1) = 0, \quad (28)$$

$$3) \quad \lim_{x \rightarrow -\infty} \psi_2'(x,z) = 0. \quad (29)$$

$$x \rightarrow -\infty$$

Prescription of the obstacle shape leads to a nonlinear boundary condition for the stream function $\psi'(x,z)$ and is consequently hard to deal with. Therefore we will again use an indirect, but exact, method for creating an obstacle and justify the procedure by the argument that the obstacle shape

is of minor importance. Indeed, the main objective of the present study is the behavior of the atmospheric flows in the lee of mountain ridges and the general characteristics of these flows should not be affected by the particular shape of the mountain profile. Two methods have been used to introduce a barrier. One is due to Yih and is a completely inverse method. A second method, due to Long, is semi-inverse in the sense that a barrier of infinitesimal height can be pre-assigned. Both methods involve the solution of Equation (26), subject to the conditions $\psi_2'(x,0) = \psi_2'(x,1) = 0$. Of course, these two conditions do not uniquely determine a solution of (26), if singularities are allowed, so long as they are located inside the barrier. Indeed, the barrier is created by these singularities.

Equation (26) is satisfied by an expression of the form

$$e^{\pm \sqrt{\lambda_n} x} f_n(z) \quad (30)$$

where λ_n is an eigenvalue of the Sturm-Liouville system

$$\frac{d^2 f}{dz^2} + \frac{1}{\gamma-1} \frac{\alpha}{1-\alpha z} \frac{df}{dz} + [\beta(1-\alpha z)^{2/\gamma-1} (Az-C) + \lambda] f = 0, \quad (31)$$

$$f(0) = f(1) = 0 \quad (32)$$

and $f_n(z)$ is the corresponding eigenfunction. The eigenvalues and corresponding orthonormal functions have been obtained by the use of power-series expansion and an iterative scheme (see Appendix II). For certain combinations of values of A and C there may be negative eigenvalues. The exponential term in (30) becomes then a sine or cosine term. All eigenfunctions are normalized according to

$$\int_0^1 \frac{f_n^2(z)}{(1-\alpha z)^{1/\gamma-1}} dz = 1. \quad (33)$$

In the first method (see [14]) the function $\psi_2'(x,z)$ is taken as an infinite series of terms of the type (30) with unknown coefficients $A_n, B_n, C_n,$ and D_n . However, the coefficients corresponding to $x < 0$ are different from the ones corresponding to $x > 0$. Furthermore, since $\psi_2'(x,z)$ has to approach zero for $x \rightarrow -\infty$, no oscillatory terms are allowed for $x < 0$, i.e., the summation for $x < 0$ begins with the first positive eigenvalue. Thus,

$$\psi_{2-}'(x,z) = \sum_{n=N+1}^{\infty} A_n e^{\sqrt{\lambda_n} x} f_n(z) \quad \text{for } x < 0, \quad (34)$$

$$\begin{aligned} \psi_{2+}'(x,z) = & \sum_{n=1}^N (B_n \cos \sqrt{-\lambda_n} x + C_n \sin \sqrt{-\lambda_n} x) f_n(z) \\ & + \sum_{n=N+1}^{\infty} D_n e^{-\sqrt{\lambda_n} x} f_n(z) \quad \text{for } x > 0, \end{aligned} \quad (35)$$

in which N is the number of negative eigenvalues of the Sturm-Liouville system consisting of (31) and (32).

Provided the series converge, both $\psi_{2-}'(x,z)$ and $\psi_{2+}'(x,z)$ satisfy Equation (26) and the conditions (27) and (28). The function $\psi_{2-}'(x,z)$, valid for $x < 0$, vanishes for $x \rightarrow -\infty$ and thus satisfies (29). The coefficients A_n, B_n, C_n and D_n will now be determined to create a barrier on the lower boundary. It should be noted that the function $\psi_2'(x,z)$, consisting of $\psi_{2-}'(x,z)$ and $\psi_{2+}'(x,z)$ is analytic for $x < 0$ and $x > 0$ ($0 \leq z \leq 1$), and the only singularities are located at $x = 0$. The fact, whether there will be singularities on the segment $x = 0$ ($0 \leq z \leq 1$) depends, of course, on the choice of the coefficients A_n, B_n, C_n and D_n . If we were to select these coefficients in such a way as to make all points $(0, 0 \leq z \leq 1)$ regular, $\psi_2'(x,z)$ would be analytic throughout the whole

strip $0 \leq z \leq 1$ and would necessarily have to be equal to zero, since periodic wave motion has been ruled by the assumption that waves do not occur far upstream. We will therefore allow the function $\psi_2'(x,z)$ to be singular on the portion $0 \leq z \leq a$ of the segment $0 \leq z \leq 1$. However, since no singularities can be tolerated in the flowfield, the created barrier should have a height of at least a at $x = 0$.

Different types of singularities can be used. For our calculations, a discontinuity in the x -derivative was introduced. Thus,

$$\psi_{2-}'(0,z) = \psi_{2+}'(0,z) \quad \text{for} \quad 0 < z < 1, \quad (36)$$

$$\frac{\partial \psi_{2-}'(0,z)}{\partial x} - \frac{\partial \psi_{2+}'(0,z)}{\partial x} = g(z) \quad \text{for} \quad 0 < z < a, \quad (37)$$

$$\frac{\partial \psi_{2-}'(0,z)}{\partial x} - \frac{\partial \psi_{2+}'(0,z)}{\partial x} = 0 \quad \text{for} \quad a < z < 1. \quad (38)$$

Equations (36) and (38) guarantee the analyticity of $\psi_2'(x,z)$ on the segment $x = 0 (a < z < 1)$ and therefore in the whole field of flow, i.e., $\psi_{2+}'(x,z)$ is the analytic continuation of $\psi_{2-}'(x,z)$ outside the barrier. The conditions (36), (37), and (38) lead to

$$\sum_{n=N+1}^{\infty} A_n f_n(z) = \sum_{n=1}^N B_n f_n(z) + \sum_{n=N+1}^{\infty} D_n f_n(z), \quad (39)$$

$$\sum_{n=1}^N \sqrt{-\lambda_n} C_n f_n(z) - \sum_{n=N+1}^{\infty} \sqrt{\lambda_n} (A_n + D_n) f_n(z) = -g(z). \quad (40)$$

It follows from (39) that

$$B_n = 0 \quad (n = 1, 2, \dots, N)$$

and

$$A_n = D_n \quad (n = N+1, N+2, \dots),$$

and from (40) that

$$\sqrt{-\lambda_n} C_n = - \int_0^1 \frac{g(z) f_n(z)}{(1-\alpha z)^{1/\gamma-1}} dz \quad (n = 1, 2, \dots, N)$$

and

$$\sqrt{\lambda_n} (A_n + D_n) = \int_0^1 \frac{g(z) f_n(z)}{(1-\alpha z)^{1/\gamma-1}} dz \quad (n = N+1, N+2, \dots) .$$

Indeed, the constants $\sqrt{-\lambda_n} C_n$ and $\sqrt{\lambda_n} (A_n + D_n)$ are merely the Fourier coefficients in the expansion of the function $g(z)$ in a series of eigenfunctions of the Sturm-Liouville system consisting of (31) and (32). The eigenfunctions corresponding to negative eigenvalues also appear in (40), i.e., all eigenfunctions must be present to make the expansion possible.

The final expressions for $\psi'_2(x, z)$ are thus

$$\psi'_{2-}(x, z) = \frac{1}{2} \sum_{n=N+1}^{\infty} \frac{Q_n}{\sqrt{\lambda_n}} e^{\sqrt{\lambda_n} x} f_n(z) \quad \text{for } x < 0 \quad (41)$$

and

$$\begin{aligned} \psi'_{2+}(x, z) = & - \sum_{n=1}^N \frac{Q_n}{\sqrt{-\lambda_n}} \sin \sqrt{-\lambda_n} x \cdot f_n(z) \\ & + \frac{1}{2} \sum_{n=N+1}^{\infty} \frac{Q_n}{\sqrt{\lambda_n}} e^{-\sqrt{\lambda_n} x} f_n(z) \quad \text{for } x > 0 , \end{aligned} \quad (42)$$

in which

$$Q_n = \int_0^a \frac{g(z) f_n(z)}{(1-\alpha z)^{1/\gamma-1}} dz .$$

The upper limit in the above integral has been taken equal to a since $g(z) = 0$ for $a < z < 1$. By changing the value of μ appearing in (25), the flow pattern can be changed. This value should be taken large enough so the barrier covers the segment $0 < z < a$ on $x = 0$. In this way the

stream function will be analytic throughout the whole field of flow. The flow pattern is given by

$$\psi'(x,z) = \psi_1'(z) + \mu\psi_{2-}'(x,z) \quad \text{for } x < 0 \quad (44)$$

and

$$\psi'(x,z) = \psi_1'(z) + \mu\psi_{2+}'(x,z) \quad \text{for } x > 0 \quad (45)$$

In the method used by Long, the field of flow is divided into three regions (see Figure 3), the middle-region (region II) containing the barrier. Although it is true that a flow pattern can be found for a barrier of arbitrary shape (however infinitesimal), we will restrict ourselves to a barrier of the shape $\frac{a}{2}(1 + \cos \frac{\pi x}{b})$. The reason for this particular choice will be pointed out later.

In each region, a homogeneous stream function is assumed each term of which satisfies Equation (26). Thus,

$$\psi_{2I}'(x,z) = \sum_{n=N+1}^{\infty} A_n e^{\sqrt{\lambda_n x}} f_n(z) \quad \text{for } x < -b, \quad (46)$$

$$\begin{aligned} \psi_{2II}'(x,z) = & F_0(z) + F_1(z) \cos \frac{\pi x}{b} + \sum_{n=1}^N (F_n \cos \sqrt{-\lambda_n} x \\ & + G_n \sin \sqrt{-\lambda_n} x) f_n(z) + \sum_{n=N+1}^{\infty} (H_n e^{\sqrt{\lambda_n} x} + M_n e^{-\sqrt{\lambda_n} x}) f_n(z) \end{aligned}$$

for $-b < x < b$, (47)

and

$$\begin{aligned} \psi_{2III}'(x,z) = & \sum_{n=1}^N (B_n \cos \sqrt{-\lambda_n} x + C_n \sin \sqrt{-\lambda_n} x) f_n(z) \\ & + \sum_{n=N+1}^{\infty} D_n e^{-\sqrt{\lambda_n} x} f_n(z) \quad \text{for } x > b. \end{aligned} \quad (48)$$

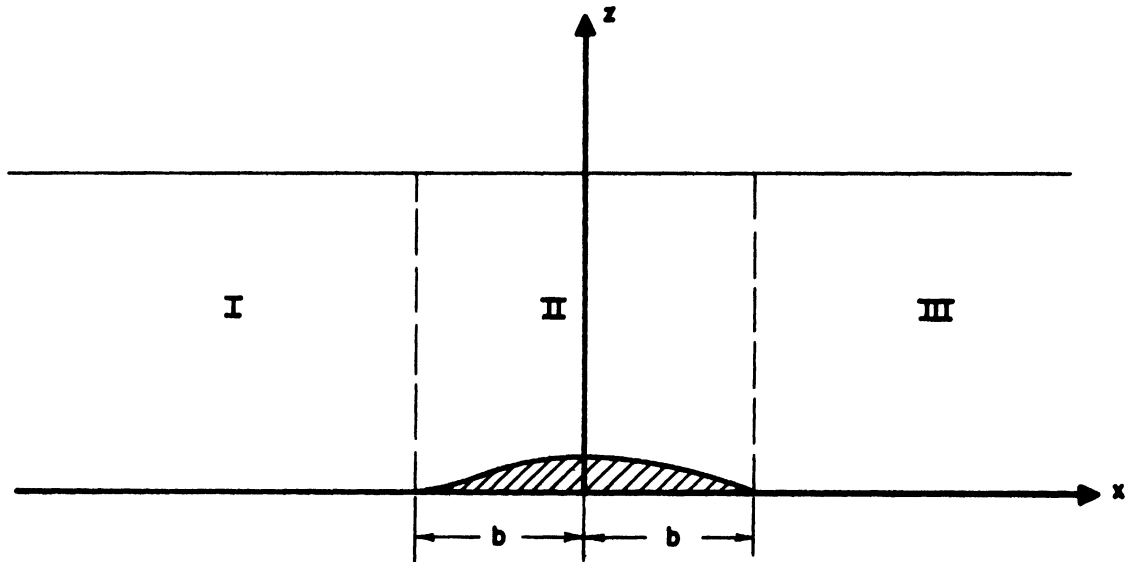


Figure 3. Flow Regions in Long's Method.

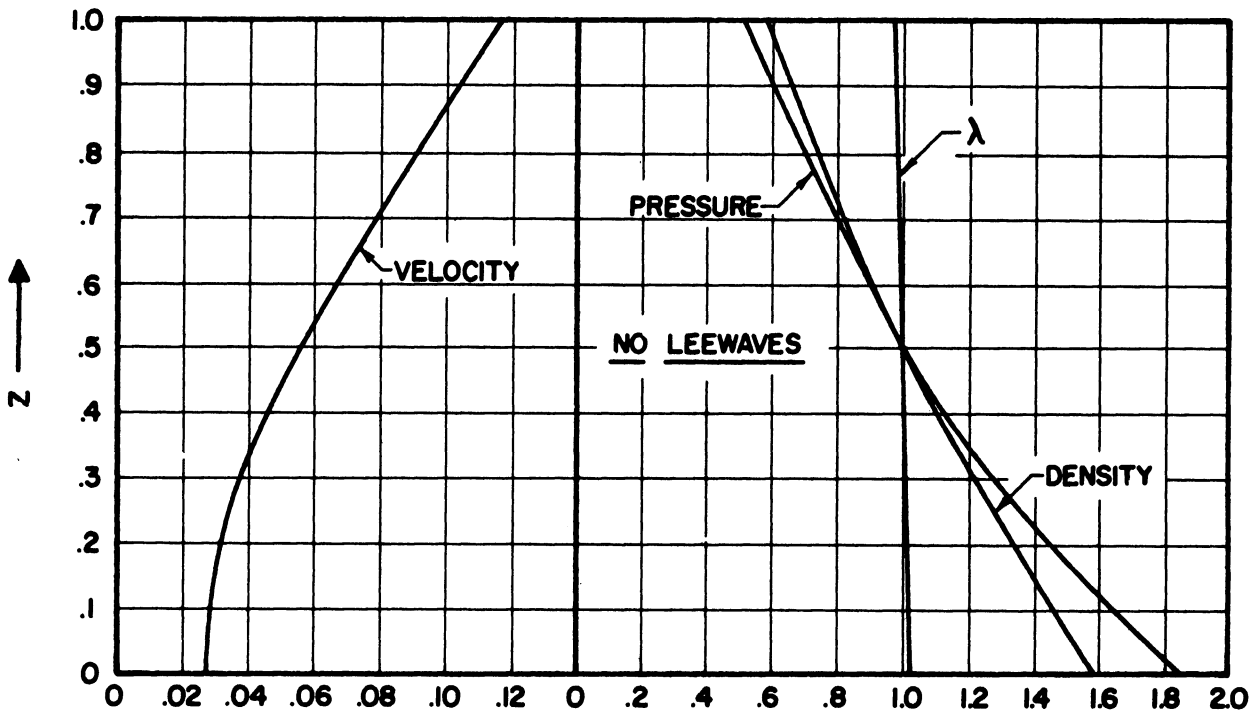


Figure 4. Upstream Conditions Leading to a Flow Pattern With No Leewave Components.

As far as regions I and III are concerned, each term in the series also satisfies the boundary condition (27), in agreement with the fact that there is no obstacle in these regions. The terms $F_0(z)$ and $F_1(z)\cos\frac{\pi x}{b}$ appearing in (47) will cause the function $\psi'_{II}(x,z)$ to be different from zero on the line $z = 0$. Therefore the line $z = 0$ will not be a stream line in region II and an obstacle is thus created. Since the functions $F_0(z)$ and $F_1(z)\cos\frac{\pi x}{b}$ have to satisfy Equation (26),

$$\frac{d^2F_0}{dz^2} + \frac{1}{\gamma-1} \frac{\alpha}{1-\alpha z} \frac{dF_0}{dz} + \beta(1-\alpha z)^{2/\gamma-1} (Az-C)F_0 = 0 \quad (49)$$

and

$$\frac{d^2F_1}{dz^2} + \frac{1}{\gamma-1} \frac{\alpha}{1-\alpha z} \frac{dF_1}{dz} + [\beta(1-\alpha z)^{2/\gamma-1} (Az-C) - \frac{\pi^2}{b^2}] F_1 = 0. \quad (50)$$

Since the upper boundary ($z = 1$) has to remain a stream line, $F_0(z)$ and $F_1(z)$ have to satisfy the conditions

$$F_0(1) = F_1(1) = 0. \quad (51)$$

Different values for $F_0(0)$ and $F_1(0)$ merely correspond to different obstacle shapes. It will be seen later that when $F_0(0)$ and $F_1(0)$ are both taken equal to 1, the convergence of the series in the Expressions (46), (47), and (48) is the fastest.

We therefore put

$$F_0(0) = F_1(0) = 1. \quad (52)$$

The integration of the Equations (49) and (50), subject to the conditions (51) and (52) is given in Appendix III. The coefficients $A_n, B_n, C_n, D_n, F_n, G_n, H_n,$ and M_n are now used to establish continuity of $\psi'(x,z)$ and

$\frac{\partial \psi'(x,z)}{\partial x}$ at the lines $x = -b$ and $x = +b$, making the function $\psi'(x,z)$ analytic throughout the whole field of flow. In order to accomplish this, the functions $F_0(z)$ and $F_1(z)$ have to be expanded in a series of eigenfunctions $f_n(z)$. Thus,

$$F_0(z) = \sum_{n=1}^{\infty} C_n^0 f_n(z) \quad (53)$$

and

$$F_1(z) = \sum_{n=1}^{\infty} C_n^1 f_n(z) . \quad (54)$$

The coefficients C_n^0 and C_n^1 are given by

$$C_n^0 = \int_0^1 \frac{F_0(z) f_n(z)}{(1-\alpha z)^{1/\gamma-1}} dz \quad (55)$$

and

$$C_n^1 = \int_0^1 \frac{F_1(z) f_n(z)}{(1-\alpha z)^{1/\gamma-1}} dz . \quad (56)$$

The integrals appearing in (55) and (56) can be evaluated easily by observing that the functions $F_0(z)$ and $F_1(z)$ satisfy the Equations (49) and (50) and the boundary conditions (51) and (52). The calculation will be carried out explicitly for C_n^0 and is analogous to the procedure followed to prove orthogonality between two distinct eigenfunctions of a Sturm-Liouville system.

Now (49) can be written as

$$\frac{d}{dz} \left[\frac{1}{(1-\alpha z)^{1/\gamma-1}} \frac{dF_0}{dz} \right] + \beta(1-\alpha z)^{1/\gamma-1} (Az-C)F_0 = 0 . \quad (49')$$

The eigenfunction $f_n(z)$ satisfies

$$\frac{d}{dz} \left[\frac{1}{(1-\alpha z)^{1/\gamma-1}} \frac{df_n}{dz} \right] + [\beta(1-\alpha z)^{1/\gamma-1} (Az-C) + \frac{\lambda_n}{(1-\alpha z)^{1/\gamma-1}}] f_n = 0 . \quad (31')$$

It follows from (49') and (31') that

$$\frac{d}{dz} \left[\frac{1}{(1-\alpha z)^{1/\gamma-1}} \left(F_0 \frac{df_n}{dz} - f_n \frac{dF_0}{dz} \right) \right] + \lambda_n \frac{F_0 f_n}{(1-\alpha z)^{1/\gamma-1}} = 0 . \quad (57)$$

Integrating Equation (57) from 0 to 1 and observing that $f_n(0) = f_n(1) = F_0(1) = 0$ and $F_0(0) = 1$, we obtain

$$\int_0^1 \frac{F_0(z) f_n(z)}{(1-\alpha z)^{1/\gamma-1}} dz = \frac{1}{\lambda_n} \frac{df_n(0)}{dz} . \quad (58)$$

Similarly, it can be shown that

$$\int_0^1 \frac{F_1(z) f_n(z)}{(1-\alpha z)^{1/\gamma-1}} dz = \frac{1}{\lambda_n + \frac{\pi^2}{b^2}} \frac{df_n(0)}{dz} . \quad (59)$$

The requirement that $\psi'(x, z)$ and $\frac{\partial \psi'(x, z)}{\partial x}$ be continuous at $x = -b$ and $x = b$ determines the values of the coefficients. These values are

$$A_n = D_n = -R_n \sinh \sqrt{\lambda_n} b \quad \text{for} \quad n > N ,$$

$$H_n = M_n = \frac{R_n}{2} e^{-\sqrt{\lambda_n} b} \quad \text{for} \quad n > N ,$$

$$B_n = 0 \quad \text{for} \quad n \leq N ,$$

$$C_n = -2R_n \sin \sqrt{-\lambda_n} b \quad \text{for} \quad n \leq N ,$$

$$F_n = R_n \cos \sqrt{-\lambda_n} b \quad \text{for} \quad n \leq N ,$$

$$G_n = -R_n \sin \sqrt{-\lambda_n} b \quad \text{for} \quad n \leq N .$$

in which

$$R_n = \int_0^1 [F_1(z) - F_0(z)] \frac{f_n(z)}{(1-\alpha z)^{1/\gamma-1}} dz ,$$

or

$$R_n = -\frac{\pi^2}{b^2} \frac{df_n(0)}{dz} \frac{1}{\lambda_n (\lambda_n + \frac{\pi^2}{b^2})} . \quad (60)$$

Equations (46), (47), and (48) become

$$\psi'_{2I}(x,z) = - \sum_{n=N+1}^{\infty} R_n \sinh \sqrt{\lambda_n b} e^{\sqrt{\lambda_n x}} f_n(z), \quad (61)$$

$$\begin{aligned} \psi'_{2II}(x,z) = & F_0(z) + F_1(z) \cos \frac{\pi x}{b} + \sum_{n=1}^N R_n \cos \sqrt{-\lambda_n} (b+x) f_n(z) \\ & + \sum_{n=N+1}^{\infty} R_n e^{-\sqrt{\lambda_n b}} \cosh \sqrt{\lambda_n x} \cdot f_n(z), \end{aligned} \quad (62)$$

$$\begin{aligned} \psi'_{2III}(x,z) = & - 2 \sum_{n=1}^N R_n \sin \sqrt{-\lambda_n} b \sin \sqrt{-\lambda_n} x f_n(z) \\ & - \sum_{n=N+1}^{\infty} R_n \sinh \sqrt{\lambda_n b} e^{-\sqrt{\lambda_n x}} f_n(z). \end{aligned} \quad (63)$$

The stream function $\psi'(x,z)$ from which the flow pattern can be obtained is then $\psi'(x,z) = \psi'_1(z) + \mu \psi'_2(x,z)$, in which $\psi'_2(x,z)$ is taken equal to $\psi'_{2I}(x,z)$, $\psi'_{2II}(x,z)$, $\psi'_{2III}(x,z)$ respectively in the regions I, II, and III.

It was mentioned earlier that the convergence of the series appearing in the Equations (46), (47), and (48) was the fastest when $F_0(0)$ and $F_1(0)$ were both taken equal to each other, say equal to 1. This should follow immediately from (58) and (59). Indeed, if $F_0(0) = a_0$ and $F_1(0) = a_1$, we would have

$$R_n = \frac{df_n(0)}{dz} \left[\frac{a_1 - a_0}{\lambda_n + \frac{\pi^2}{b^2}} - a_0 \frac{\pi^2}{b^2} \frac{1}{\lambda_n (\lambda_n + \frac{\pi^2}{b^2})} \right].$$

Unless $a_1 = a_0$, the above expression contains the term $\frac{a_1 - a_0}{\lambda_n + \frac{\pi^2}{b^2}}$ which would be responsible for the slower convergence.

The question of the rapidity of the convergence is of paramount importance since each calculation of an eigenfunction involves considerable

numerical labor. It may therefore be worthwhile to compare Yih's and Long's method in that respect.

In Yih's solution, the rapidity of the convergence is essentially determined by the integrals $\left\{ \int_0^a \frac{g(z)f_n(z)}{(1-\alpha z)^{1/\gamma-1}} dz \right\}$. The behavior of this sequence depends of course on the choice of the function $g(z)$ creating the singularity. However, one can generally state that, the smaller the upper limit a becomes, the worse the convergence is. But creating a low barrier necessarily leads to a small value of a , since the singularities cannot extend into the field of flow. The method is thus not favorable for obtaining flows over very low barriers.

It has already been pointed out that the height of the barrier does not affect the rapidity of convergence in Long's method which can thus favorably be used for obtaining flows over low barriers. However, the convergence is affected by the width of the obstacle. Indeed, when b is small (short obstacle) the term π^2/b^2 is large and the expression $\frac{1}{\lambda_n(\lambda_n + \frac{\pi^2}{b^2})}$ behaves essentially as $1/\lambda_n$ for λ_n not too large. Furthermore, the value of $df_n(0)/dz$ is of the order $\sqrt{\lambda_n}$. Thus the coefficient R_n given by (60) behaves like $1/\sqrt{\lambda_n}$. Therefore, in order to obtain a sufficiently accurate representation of the solution, many more terms have to be taken than in the case of a long obstacle. Indeed, if b is large (long obstacle), the coefficient R_n behaves like $1/\lambda_n \sqrt{\lambda_n}$ after only very few terms. From a practical point of view the method of Long is not preferable for flows over short barriers.

V. DISCUSSION OF RESULTS

The reference point, at which the pressure and density are equal to p_0 and ρ_0 respectively, has been chosen in the middle of the troposphere, that is at $z = 0.5$. The following values have been taken for p_0 and ρ_0 :

$$p_0 = 410 \text{ mm Hg} ,$$
$$\rho_0 = .000723 \text{ gram/cm}^3 .$$

The height of the tropopause has been taken to be 10 km. The average value of the specific energy H' used in the calculations was obtained by evaluating this quantity at the reference point $z = 0.5$.

$$H' = 3.198 + \frac{U^2}{2} = 3.2 .$$

With $\gamma = 1.4$, the coefficients α and β then become

$$\alpha = 0.3125 ,$$
$$\beta = 2.3471 .$$

With the above numerical values, several upstream conditions have been obtained. The density, pressure and temperature profiles approximate the realistic profiles in the atmosphere closely. This is hardly surprising if one considers the fact that the stratifications in entropy and specific energy occurring in the atmosphere are rather slight and we have chosen the constants A , B , C , and D in such a way as to make these latter conditions satisfied. Although the velocity term ($U'^2/2$) was included in Equation (23) to determine the pressure variation (with height), quite large velocity changes have a rather limited influence on the pressure profile. Various upstream conditions (including the wind profiles) corresponding

to various wave formations in the lee are shown in Figures 4, 6, and 10. All the examples shown correspond to an entropy increasing with height (or λ decreasing with height), as is required by static stability (see Section 6). The essential task is to find some combinations of stratifications in entropy and specific energy together with compatible velocity profiles that give rise to either no leewaves or leewaves with one or more components. By reducing the velocity far upstream and leaving the other quantities unaltered, it is possible to create more leewave components. Indeed, once A and C are chosen the number of leewave components (corresponding to the negative eigenvalues) is fixed. Decreasing the velocity, which is equivalent to reducing the stream function, then results in a smaller stratification. The extreme case (zero velocity upstream and no stratification) can be considered as the limit case of a flow with several wave components in the lee.

Figure 5 shows a flow pattern with no waves in the lee. The obstacle is symmetric, as expected. The solution has been obtained by Yih's method. Mathematically, a solution is allowed for any height of the obstacle in agreement with the fact that there are no leewaves present. Indeed, once a particular height h of the obstacle has been selected the coefficient μ appearing in (25) is given by

$$\mu = - \frac{\psi_1'(h)}{\psi_2'(0,h)} . \quad (64)$$

If $\psi_2'(x,z)$ does not have any nodal lines and therefore $\psi_2'(0,z) \neq 0$ for $0 < z < 1$, Equation (64) yields a value of μ for any height h between 0 and 1. In the case of one leewave component (say), the function $\psi_2'(x,z)$

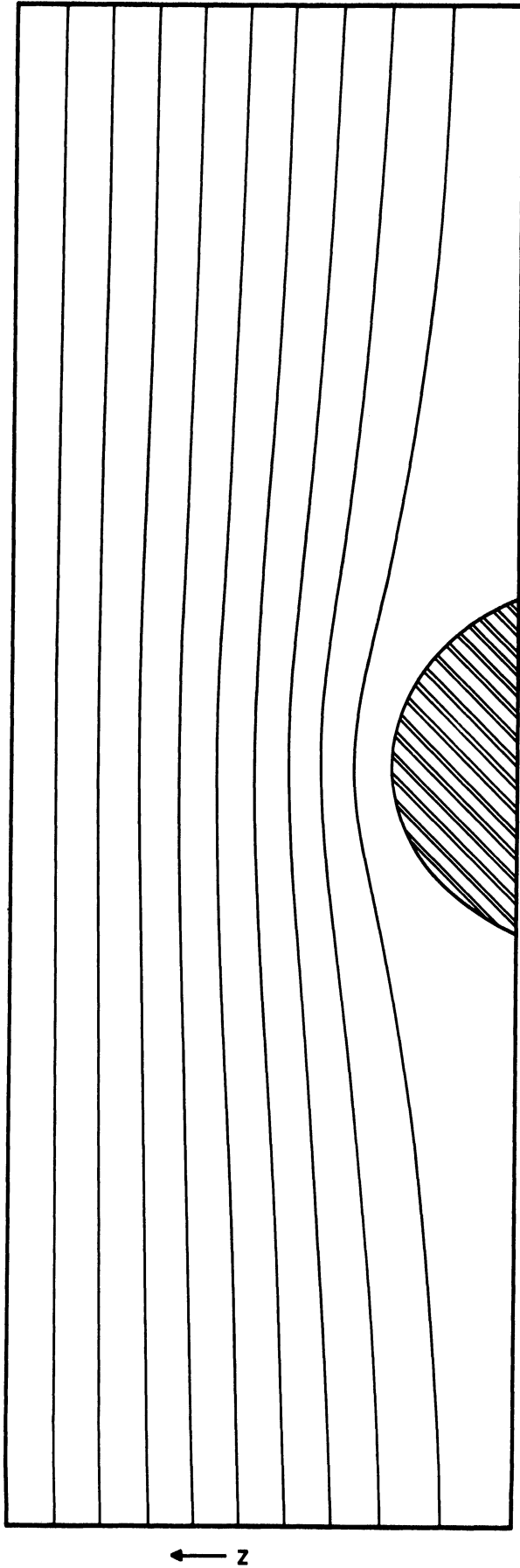


Figure 5. Flow Pattern With No Loewaves.

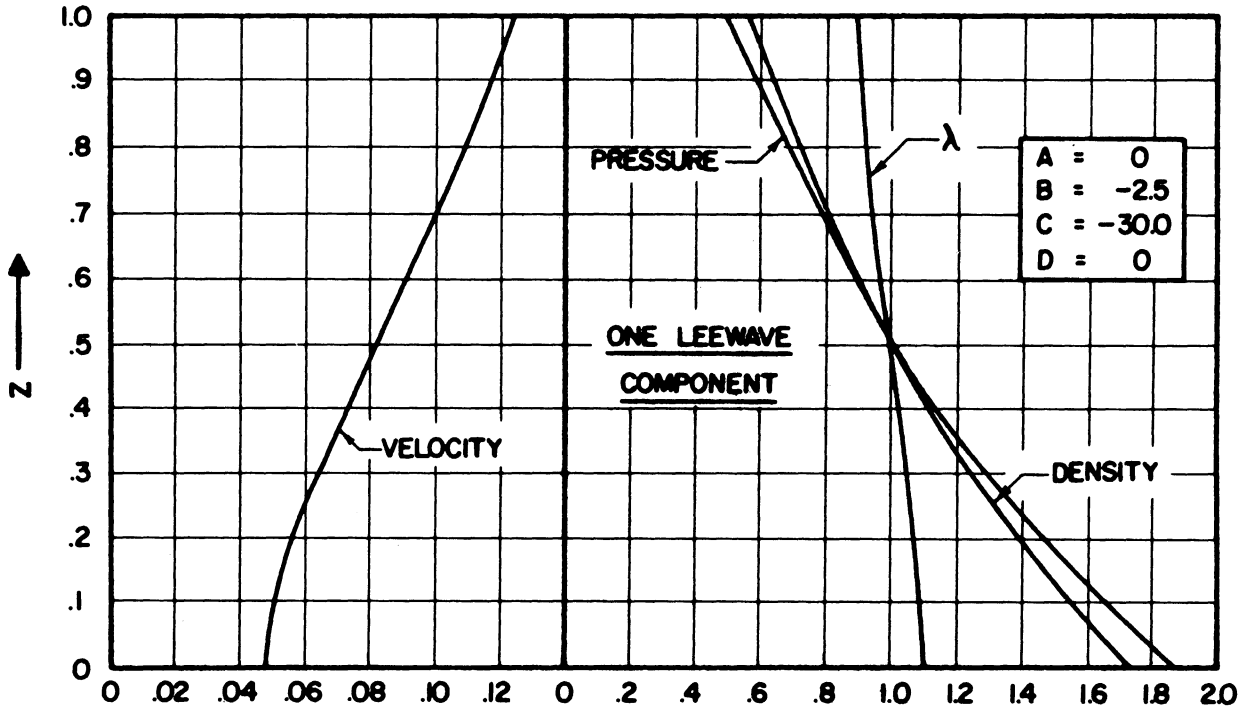


Figure 6. Upstream Conditions Leading to a Flow Pattern With One Leewave Component.

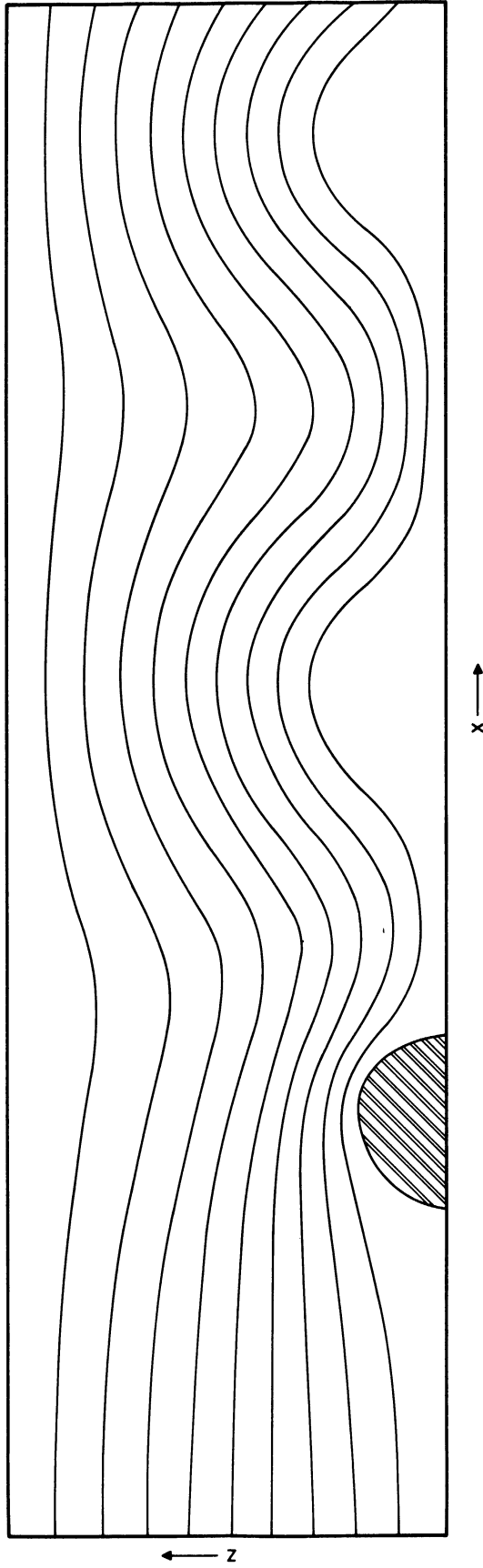


Figure 7. Flow Pattern With One Leeward Component.

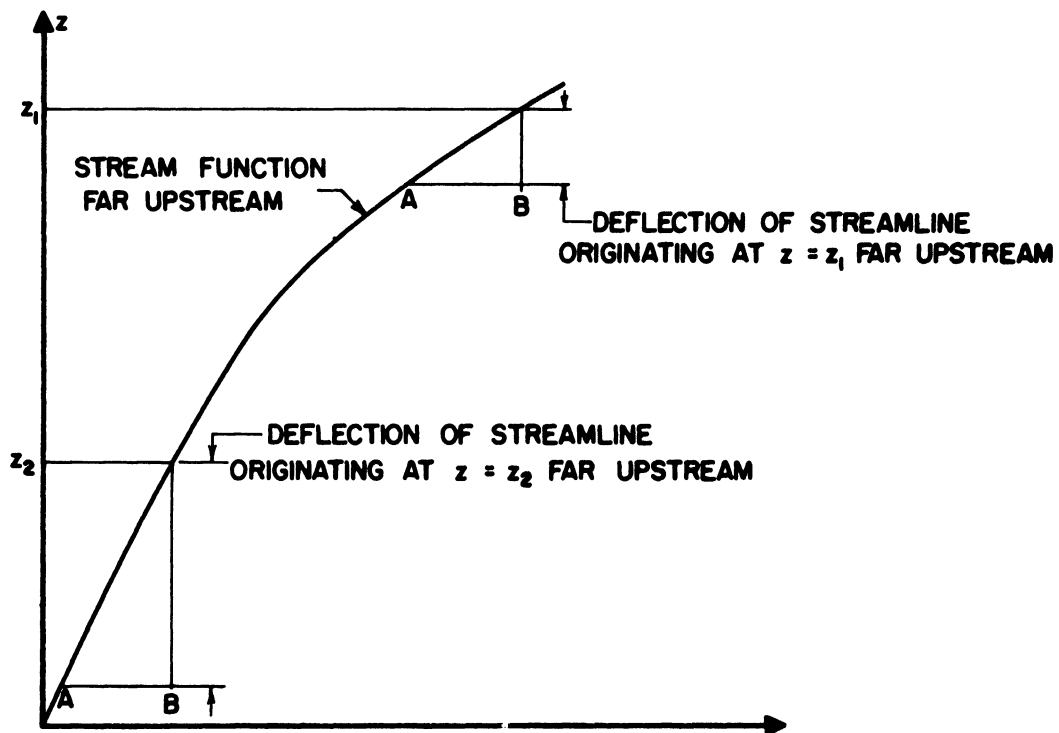


Figure 8. Influence of Wind Profile on Wave Amplitude.

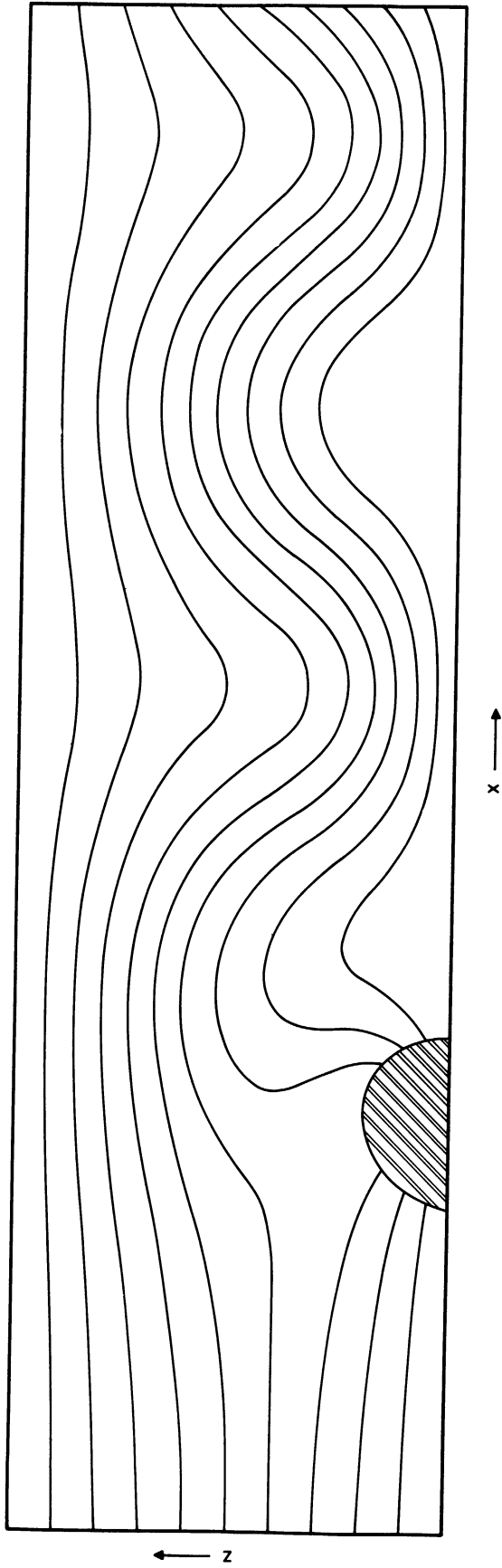


Figure 9. Isothermal Lines in the Flow With One Leeward Component.

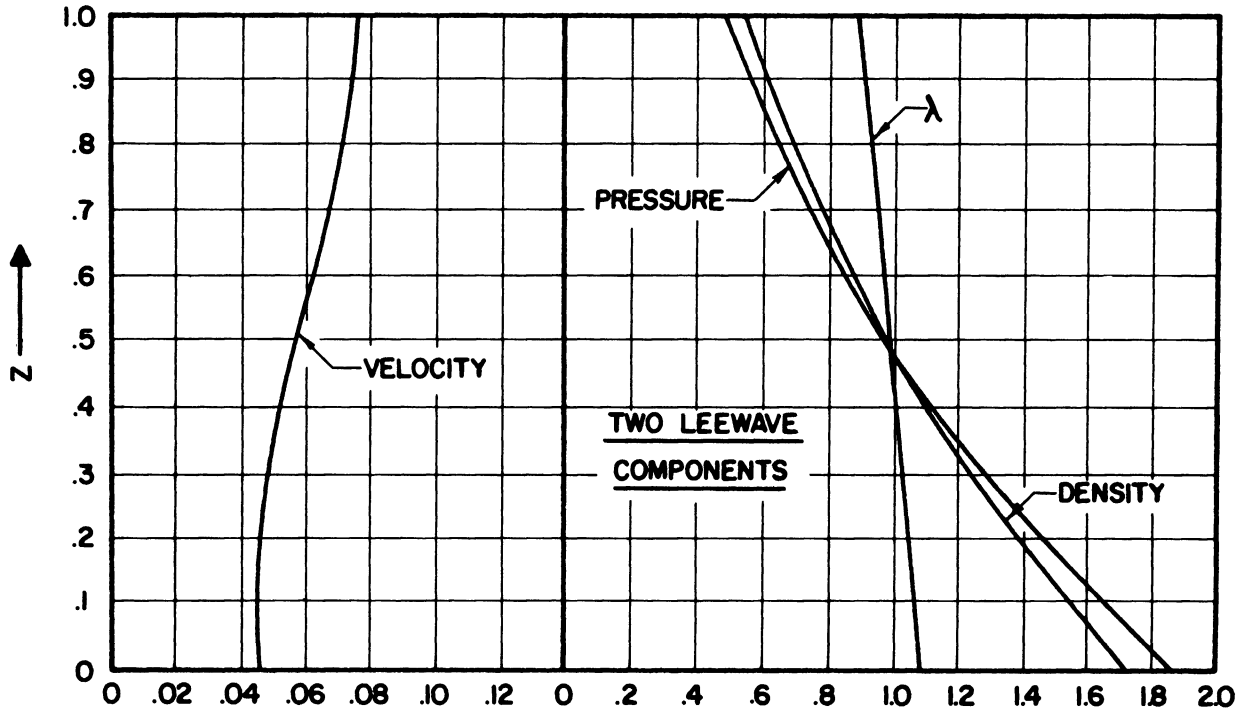


Figure 10. Upstream Conditions Leading to a Flow Pattern With Two Leewave Components.

has one nodal line and there exists a number z_1 between 0 and 1 such that

$$\psi_2'(0, z_1) = 0 .$$

Equation (64) still yields a value on μ provided $h < z_1$. The obstacle height approaches z_1 , as μ approaches infinity. It is thus impossible to obtain a steady flow past an obstacle of a height greater than the height of the nodal line.

Figure 7 represents a flow pattern where the coefficients A and C have been selected to give rise to one wave component in the lee. The usual jet occurring above the barrier and extending upstream is present. The much stronger wave motion in the lower part of the channel should not be considered merely (if at all) as a result of compressibility. One of the reasons certainly is the shape of the velocity profile far upstream. It may be conjectured that a higher velocity in the upper part of the channel has a "washing down" effect on the waves. Indeed, as pointed out earlier, increasing the velocity by constant stratification tends to eliminate wave motion. The influence of the velocity profile on the development of the waves as a function of height may become clearer by the following consideration. If the velocity increases with height, the graph representing the stream function $\psi_1'(z)$ upstream is curved downward (see Figure 8). This means that a moderate value (represented by the segment AB in Figure 8) of the stream function $\psi_2'(x, z)$ will cause a rather large deflection of the relevant streamline when one considers the lower part of the channel, while the same value of $\psi_2'(x, z)$ would only cause a small deviation in the upper part of the channel. This would indicate that such a velocity profile (velocity increasing with height) favors the wave development near the

ground. The opposite conclusions are reached if velocity profiles are considered where the velocity decreases with height.

The isothermal lines corresponding to the flow of Figure 7 are shown in Figure 9. The temperature can easily be calculated from

$$T = \frac{H' - \lambda z}{\lambda E}, \quad (65)$$

in which the velocity term has been neglected. It can be seen from the Figures 7 and 9 that an air particle in its up and down motion will have a varying temperature. These temperature changes are, of course, due to isentropic compression and expansion. A short numerical calculation reveals that the temperature of a particle following the lower streamline (originating at $z = 0.1$ far upstream) changes from 15°C to -11°C . This partially explains the formation of equally spaced clouds as has sometimes been observed in the lee of mountain ridges. If the humidity of the air is such that the saturation point is reached in the vicinity of the crests of the waves, apparently stationary clouds would be formed. However, in the case of humid air, the results are only qualitatively true since the basic assumption, $\lambda = \text{constant}$ along a streamline, becomes questionable when the medium undergoes a partial change of state.

Figure 11 shows a pattern with two leewave components and was obtained using Long's method. The formation of two jets, one downward and one upward, is apparent. The downward jet is more developed for reasons pointed out earlier. Although no closed cells appear, they could be created by increasing the height of the obstacle. However, the flow inside these cells, as obtained by previous analysis, is not a priori justifiable because the

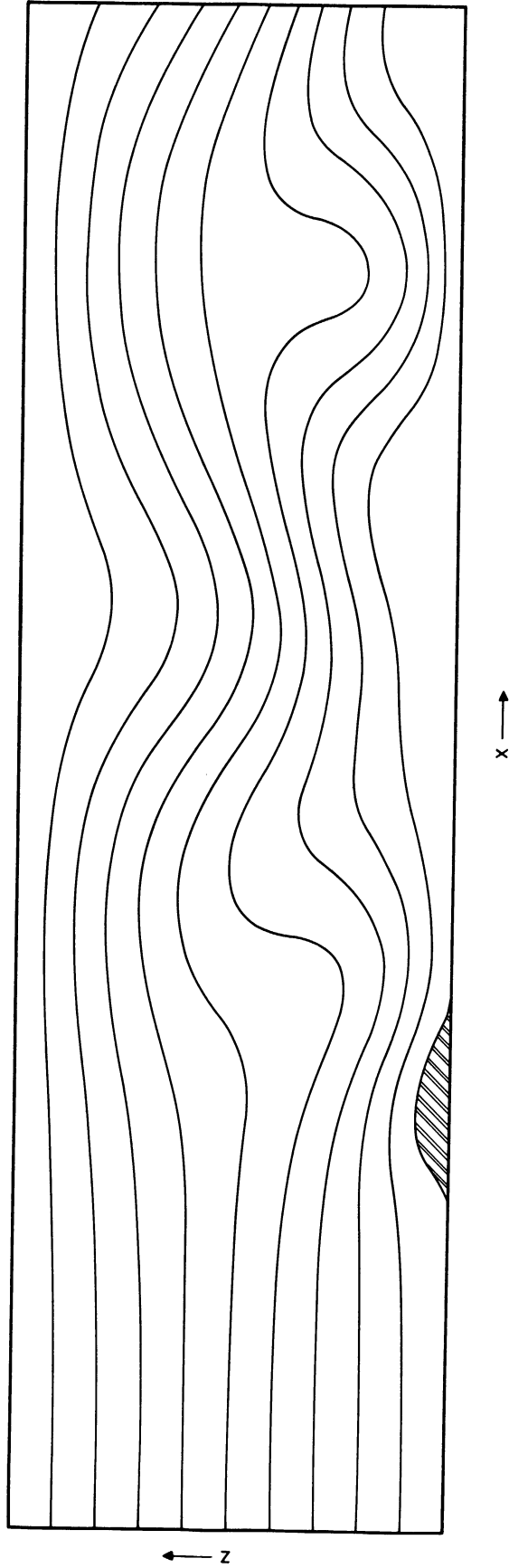


Figure 11. Flow Pattern With Two Leeway Components.

streamlines in the eddies do not originate far upstream and consequently the upstream conditions do not determine the values of λ and H' on these streamlines. Care has been taken to keep the obstacle height below a certain limit in order to avoid extremely converging streamlines since these would lead to high velocities and the validity of neglecting the dynamic compressibility might come into play.

VI. COMPARISON WITH FLOW OF AN INCOMPRESSIBLE FLUID

In order to bring out the effect of compressibility an attempt has been made to obtain a flow of a compressible fluid and a flow of an incompressible fluid, both with equivalent upstream conditions (what is meant here by "equivalent" will be explained later). We know that for the governing differential system to be linear, an inverse procedure has to be adopted as indicated in Section 3. This makes a complete match of upstream conditions of two different flows (compressible and incompressible) impossible. Since the theory dealing with the flow of an incompressible stratified fluid will be needed, a brief summary of the equations in dimensionless form is given below. For more details we refer to [14]. The associated velocity field (u', w') is related to the original velocity field (u, v) by means of

$$u' = u \sqrt{\rho} \quad \text{and} \quad w' = w \sqrt{\rho} \quad .$$

These two velocity components (u', w') can be derived from the stream function $\psi'(x, z)$ by

$$u' = \frac{\partial \psi'}{\partial x} \quad \text{and} \quad w' = - \frac{\partial \psi'}{\partial z} \quad .$$

The stream function satisfies the equation

$$\nabla^2 \psi' + z \frac{d\rho}{d\psi'} = \frac{dH'}{d\psi'} \quad , \quad (66)$$

in which

$$H' = p + \frac{\rho}{2} (u^2 + w^2) + \rho z \quad . \quad (67)$$

Equation (66) can again be made linear by assuming linear functions of ψ' for $d\rho/d\psi'$ and $dH'/d\psi'$. The most general, but linear, case leads to

Bessel functions of fractional order. In some cases, however, the solution can be expressed in terms of trigonometric and exponential functions. This is the case when far upstream we choose the density as a linear function of height, and the associated velocity equal to a constant. Thus, far upstream the conditions are prescribed by

$$\begin{aligned} \rho &= 1 + a (1-2z) , \\ U' &= U'_0 , \end{aligned} \tag{68}$$

where a and U'_0 are constants as indicated on Figure 12. Then

$$\psi'_1 = U'_0 z$$

and

$$\frac{d\rho}{d\psi'} = \frac{d\rho}{dz} \frac{1}{U'_0} = - \frac{2a}{U'_0} . \tag{69}$$

The term $dH'/d\psi'$ becomes

$$\frac{dH'}{d\psi'} = \frac{1}{U'_0} \frac{dH'}{dz} = \left(\frac{d\rho}{dz} + \rho + z \frac{d\rho}{dz} \right) \frac{1}{U'_0} = z \frac{d\rho}{dz} \frac{1}{U'_0} .$$

So, with $\frac{d\rho}{dz} = -2a$ by virtue of (68),

$$\frac{dH'}{d\psi'} = - \frac{2a}{U'_0} z = - \frac{2a}{U'^2_0} \psi' . \tag{70}$$

Far upstream, Equation (66) becomes

$$\frac{d^2\psi'_1}{dz^2} + \frac{2a}{U'^2_0} \psi'_1 = \frac{2az}{U'_0} . \tag{71}$$

The general solution is

$$\psi'_1(z) = C_1 \sin \left(\frac{\sqrt{2a}}{U'_0} z + C_2 \right) + U'_0 z . \tag{72}$$

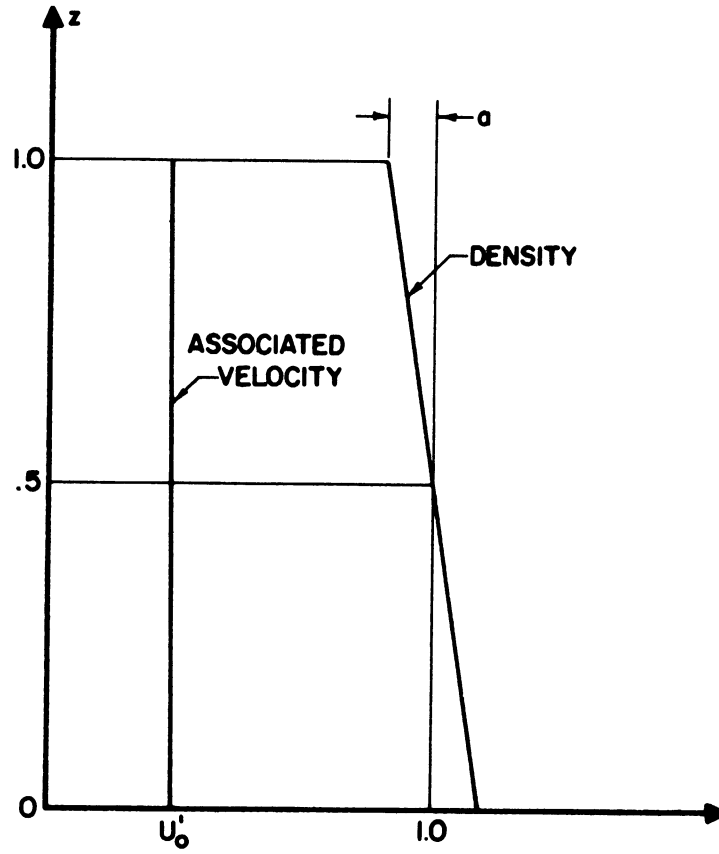


Figure 12. Upstream Conditions for an Incompressible Fluid and Leading to Equation (71).

The velocity U' is given by

$$U'(z) = \frac{\sqrt{2a}}{U'_0} [C_1 \cos \left(\frac{\sqrt{2a}}{U'_0} z + C_2 \right)] + U'_0 \quad . \quad (73)$$

We see that, although Equation (71) was obtained from a linear density stratification and constant associated velocity far upstream, a whole class of velocity profiles, given by (73), and corresponding density stratifications lead to the same differential equation for the stream function. Furthermore, any arbitrary constant may be added to the stream function and will not change the velocity profile. The stream function is then governed by an equation which differs from Equation (71) by a constant in the right-hand member. This flexibility will be used to get a closer match between the incompressible and compressible flow.

By adjusting the value of the coefficients A , B , C , and D in the case where compressibility is taken into account, a velocity profile (see Figure 13) has been obtained which can be matched closely by a function of the form given by (73). The density variation is of course considerable and corresponds roughly to normal atmospheric conditions. If we use an incompressible fluid in an attempt to describe the flow of a compressible one, there is some question as to what density stratification should be taken far upstream. It is indeed the combined action of density difference and gravity that determines the restoring forces necessary for the creation of waves. The fact that the same density stratification in both compressible and incompressible fluid will give rise to different restoring forces can easily be inferred from the following reasoning. The density of a particle of air increases as the particle goes down (due to compression) and decreases when it goes up (due to expansion), whereas the density of a particle of an incompressible

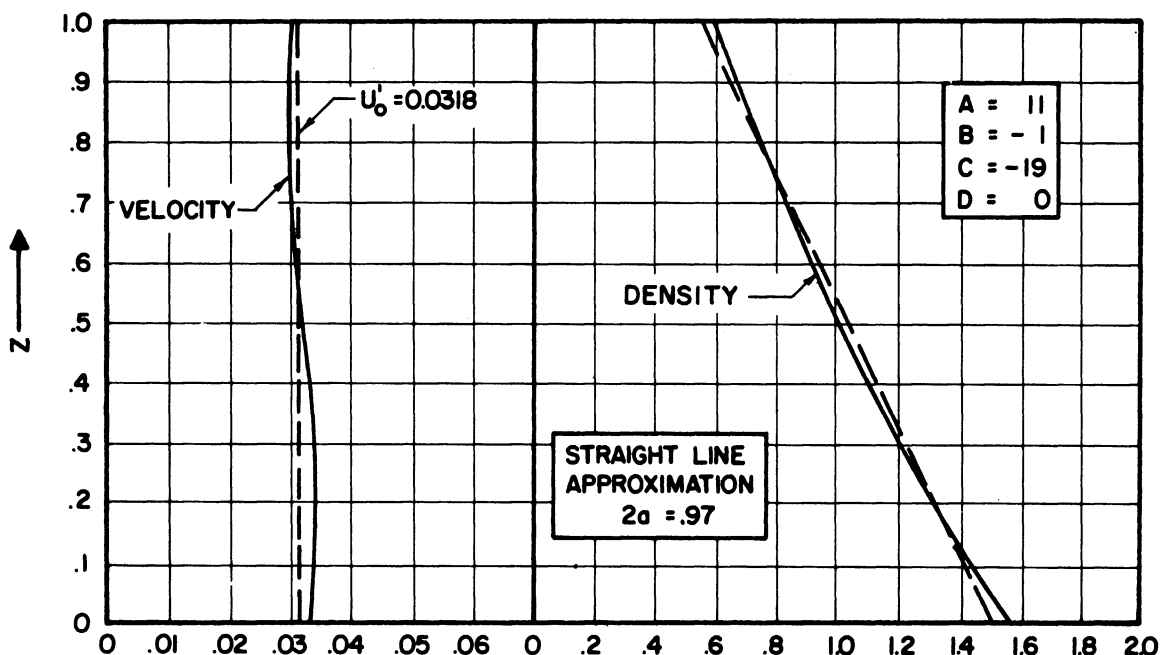


Figure 13. Upstream Conditions Used for the Comparison Between the Flow of an Incompressible Fluid and the Flow of a Compressible Fluid.

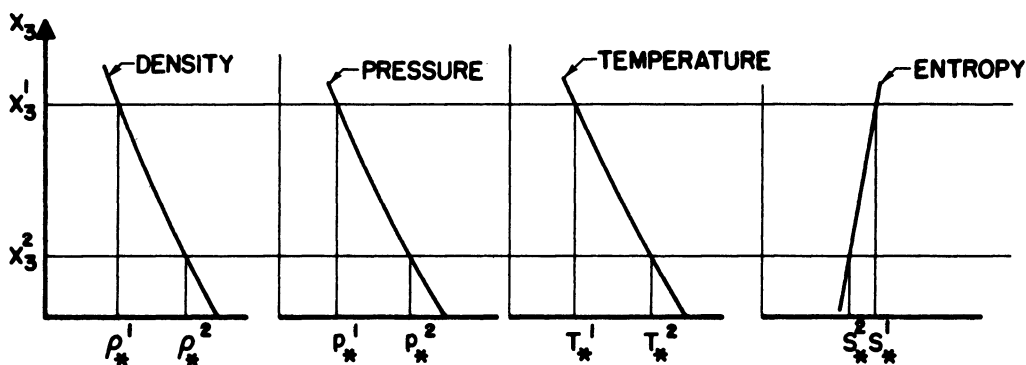


Figure 14. Stratification of Density, Pressure, Temperature and Entropy in the Atmosphere and Illustrating the Concept of Potential Density.

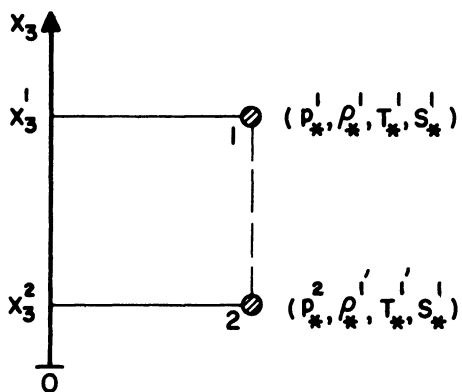


Figure 15. Relocation of a Particle in a Quiescent Atmosphere Illustrating the Concept of Potential Density.

fluid is independent of the surrounding pressure and thus independent of its location.

Besides, the following numerical calculation already predicts the marked difference in behavior between the flow of a compressible and an incompressible fluid, the density stratification being taken equal in both cases.

If we roughly approximate the density stratification, as shown in Figure 13, by a straight line and the velocity profile by a constant, we get for the values of a and U'_0 appearing in Equation (71)

$$a = 0.485 \quad \text{and} \quad U'_0 = 0.0318 .$$

Equation (71) then becomes

$$\frac{d^2 \psi'_1}{dz^2} + 959 \psi'_1 = 30.5z .$$

This indicates that the resulting flow pattern would contain 9 leewave components while the corresponding flow of the fluid being considered compressible contains only a single wave component! In order to find the appropriate density stratification (for an incompressible fluid) we have to introduce the concept of potential density.

In order to get a clear picture of this concept we consider an ideal compressible fluid at rest in which a certain density stratification $\rho_*(x_3)$ prevails (Figure 14). From this density $\rho_*(x_3)$ follows the pressure $p_*(x_3)$ according to the law of hydrostatics. The gas law then provides the temperature $T_*(x_3)$. Any function of state (i.e., only depending on the thermodynamic coordinates p_*, ρ_*, T_*) can now be evaluated at any height.

In particular the entropy S_* is shown in Figure 14. The thermodynamic coordinates at the heights x_3^1 and x_3^2 will be denoted by p_*^1, ρ_*^1, T_*^1 and p_*^2, ρ_*^2, T_*^2 respectively. We will take a particle located at $x_3 = x_3^1$ and move it isentropically, by some means, to a new location, say $x_3 = x_3^2$ (Figure 15). The particle, originally having the thermodynamic coordinates p_*^1, ρ_*^1, T_*^1 has now acquired the coordinates $p_*^2, \rho_*^{1'}, T_*^{1'}$ and its entropy (S_*^1) has remained unchanged. The pressure prevailing in the particle should indeed be the same as that of its new surroundings, i.e., pressure p_*^2 . The quantities $\rho_*^{1'}$ and $T_*^{1'}$ are obtained by letting the particle complete an isentropic change of state from pressure p_*^1 to pressure p_*^2 . If the density $\rho_*^{1'}$ is different from the density of its new surroundings, i.e., different from ρ_*^2 , there will be a net force (buoyancy) acting on the particle. If w is its weight and ΔV and $\Delta V'$ its volume in position 1 and position 2 respectively, the buoyancy force F is

$$F = g\rho_*^2\Delta V' - w .$$

The force f per unit weight is

$$f = \frac{F}{w} = \frac{\rho_*^2}{\rho_*^{1'}} - 1 , \quad \text{since} \quad w = g\rho_*^{1'}\Delta V' .$$

In order to find an expression of $\frac{\rho_*^2}{\rho_*^{1'}}$ in terms of the entropies S_*^1 and S_*^2 , we apply the relationship

$$\frac{\rho_*}{\rho_0} = \left(\frac{p_*}{p_0}\right)^{1/\gamma} e^{S_0 - S_*/C_p}$$

(p_0, ρ_0, S_0 taken at a reference point) successively to the particle in

position 2 and to any fluid particle originally at position 2. Thus,

$$\frac{\rho_*^{1'}}{\rho_o} = \left(\frac{p_*^2}{p_o}\right)^{1/\gamma} e^{S_o - S_*^1/C_p} \quad (74)$$

and

$$\frac{\rho_*^2}{\rho_o} = \left(\frac{p_*^2}{p_o}\right)^{1/\gamma} e^{S_o - S_*^2/C_p} . \quad (75)$$

Division of (75) by (74) produces

$$\frac{\rho_*^2}{\rho_*^{1'}} = e^{S_*^1 - S_*^2/C_p} .$$

The buoyancy force per unit weight becomes

$$f = e^{S_*^1 - S_*^2/C_p} - 1. \quad (76)$$

Now for an incompressible fluid, as a particle originally at the height x_3^1 is moved to the height x_3^2 , the buoyancy force per unit weight (f_i) that the particle experiences in its new location (at $x_3 = x_3^2$) will depend on the density stratification. We demand that this stratification is such that the force f_i is the same as in the previous case of the compressible fluid, i.e., $f_i = f$. The density

$$\rho_{*i} = \rho_o e^{S_o - S_*/C_p} \quad (77)$$

will satisfy this requirement. Indeed, the buoyancy force f_i per unit weight is

$$f_i = \frac{\rho_{*i}^2}{\rho_{*i}^1} - 1 = e^{S_*^1 - S_*^2/C_p} - 1 .$$

which is identical to (76). The density ρ_{*i} given by (77) is called the potential density and corresponds to a certain entropy stratification $S_*(x_3)$ in the compressible fluid.

The potential density can be written in the dimensionless form

$$\frac{\rho_{*i}}{\rho_0} = e^{(S_0 - S_*)/C_p} = \frac{\rho_*}{\rho_0} \left(\frac{p_0}{p_*}\right)^{1/\gamma} = \lambda .$$

When flows of a compressible and an incompressible fluid were compared, it was pointed out earlier that the assumption of the same density stratification far upstream led to entirely different flow patterns. The reason for this is that the action of gravity in the case of the compressible fluid is not correctly accounted for when the former assumption is adopted. It follows from the previous discussion on potential density that the latter is a more realistic density stratification for the incompressible fluid. It is indeed only in this case that the restoring forces will be close to the ones occurring in the compressible flow.

In the case of the incompressible fluid, an ideal choice of the upstream conditions consists of a velocity profile identical to the velocity profile in the compressible flow (Figure 13), and a density stratification identical to the potential density stratification (Figure 16) prevailing in the compressible fluid.

The above quantities can be approximated rather closely by taking

$$a = 0.01345, \quad U'_0 = 0.0318, \quad C_1 = 0.000318 \quad \text{and} \quad C_2 = -1.0315$$

in Equation (73). The velocity profile is then given by

$$U'(z) = 0.00164 \cos (5.1576z - 1.0315) + 0.0318.$$

This profile is so close to the one shown in Figure 13 that the two graphs practically coincide. The stream function has been evaluated from

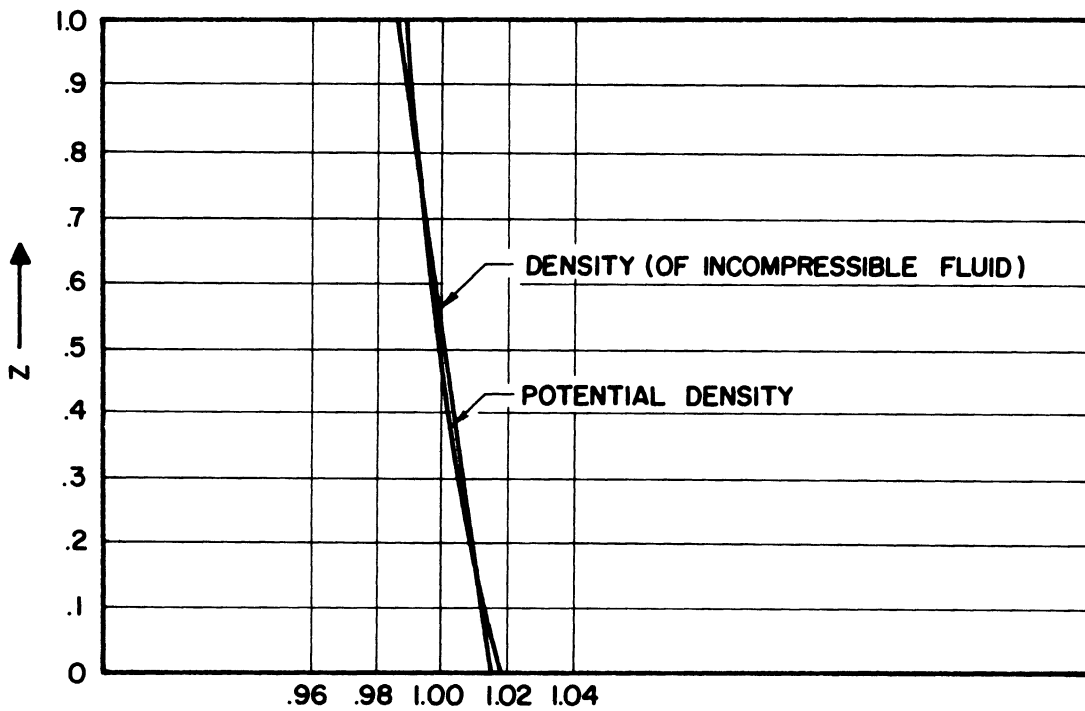


Figure 16. Approximation of the Stratification of Potential Density in a Compressible Fluid by the Density Stratification in an Incompressible Fluid. Both Stratifications Lead to Linear Governing Equations.

Equation (72) and is given by

$$\psi_1'(z) = 0.000318 \sin(5.1576z - 1.0315) + 0.0318z .$$

The density stratification then is

$$\rho(z) = -\frac{2a}{U_0'} \psi_1'(z) + \text{Constant} = -0.8459 \psi_1'(z) + 1.0157 .$$

The above stratification is almost linear and is shown, as a basis for comparison, in Figure 16. Inserting the numerical values of a and U_0' in the Expressions (69) and (70), we obtain

$$\frac{d\rho}{d\psi_1'} = -0.8459 \quad \text{and} \quad \frac{dH'}{d\psi_1'} = -26.601\psi_1' .$$

Equation (66) becomes

$$\nabla^2 \psi_1' + 26.601\psi_1' = 0.8459z . \quad (78)$$

The resulting flow pattern has been obtained by Long's method since this method allows us to control both the width and the height of the obstacle (Figure 17). The corresponding flow pattern of the compressible fluid is shown in Figure 18.

The Sturm-Liouville system resulting from the separation of variables in Equation (78) admits one negative eigenvalue and hence, one leewave component is present in the flow pattern. It is interesting that the negative eigenvalue in the case of the compressible fluid is nearly equal to the negative eigenvalue corresponding to the incompressible flow. Indeed the latter is

$$\lambda_1 = \pi^2 - 26.601 = -16.731$$

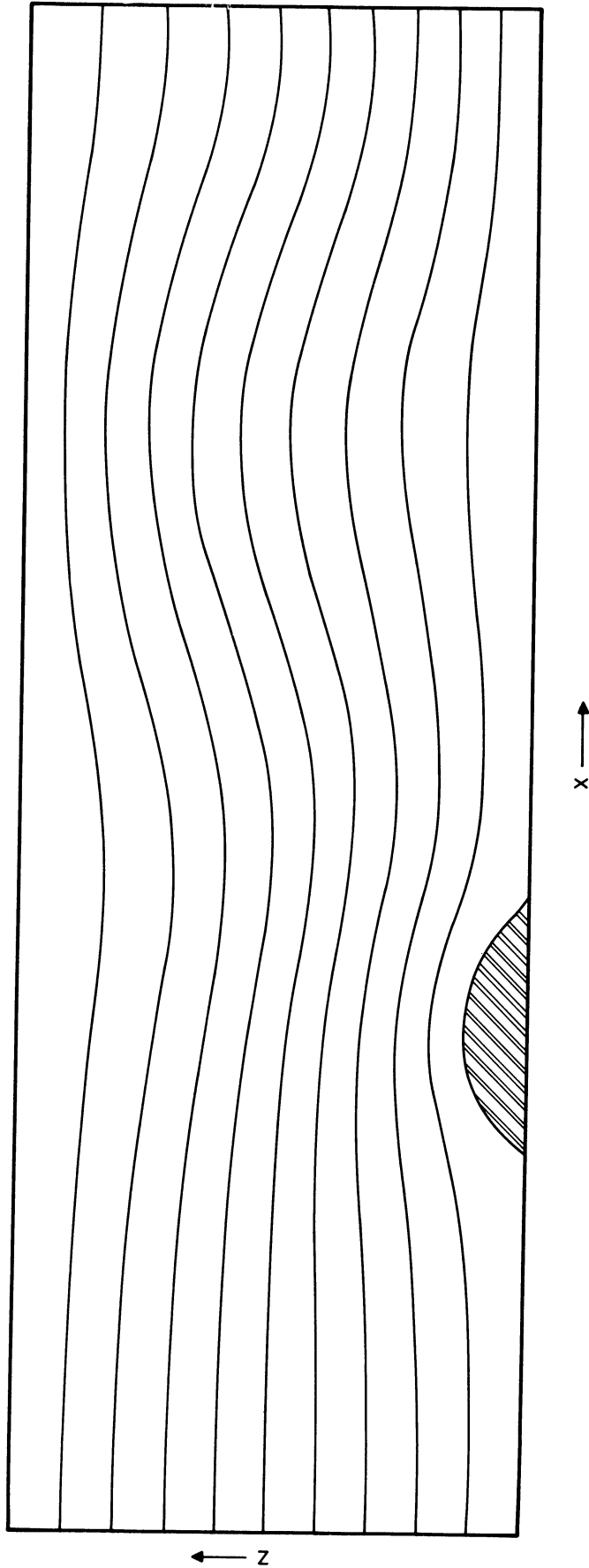


Figure 17. Comparison Between the Flow of an Incompressible and a Compressible Fluid.
Incompressible Case

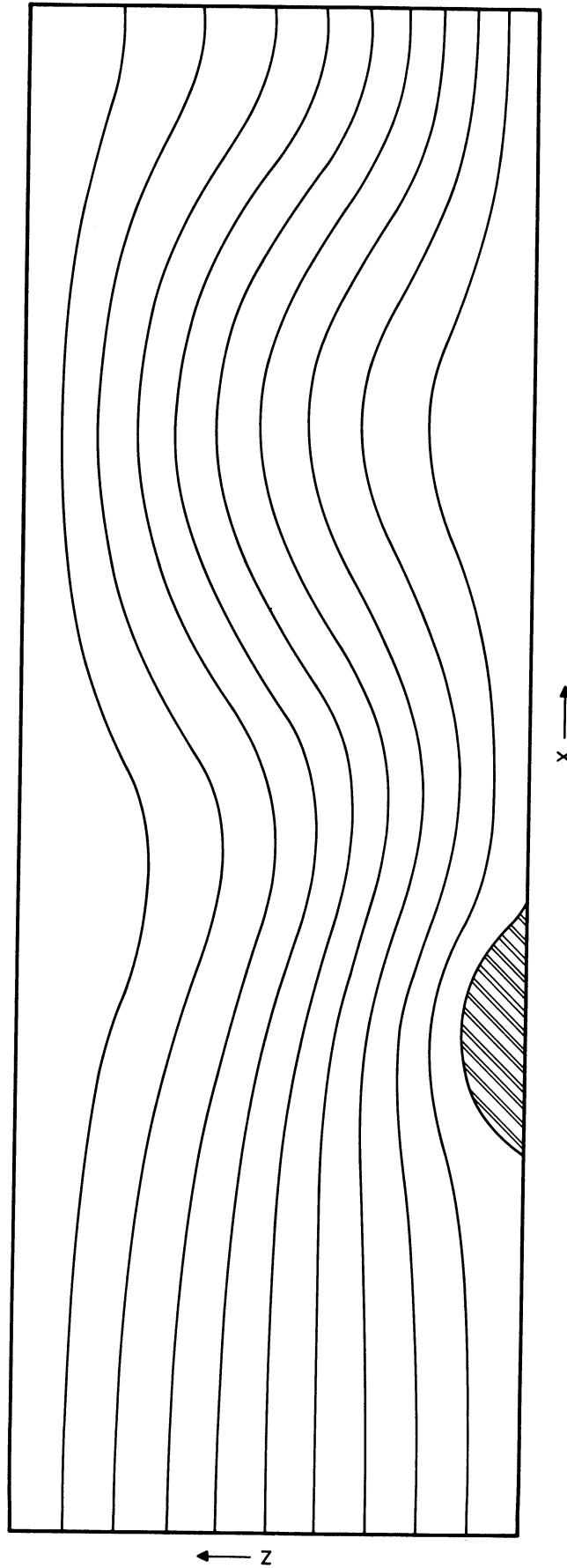


Figure 18. Comparison Between the Flow of an Incompressible and a Compressible Fluid.
Compressible Case

while the corresponding numerical value in the case of the compressible fluid was found to be -16.078 . This means that the wave lengths in both flow patterns are nearly equal as can be seen from Figures 17 and 18. However, in spite of the fact that the obstacles in both cases (compressible and incompressible) are nearly equal, the wave motion is of larger amplitude in the case of the compressible fluid. Indeed, the maximum vertical oscillation of a streamline in the compressible flow is approximately 0.29 whereas the corresponding oscillation in the incompressible flow is roughly 0.165 . The jet extending upstream is markedly more convergent in the compressible flow than in the incompressible one.

It is interesting to observe the behavior of the lower streamline (originating at $z = 0.1$ far upstream) in both cases. Both streamlines have approximately the same shape upstream of the trailing edge of the obstacle. Downstream from the obstacle however, the maximum vertical oscillation of this streamline is, in the case of the compressible fluid, more than 3 times as large as the corresponding oscillation in the case of the incompressible fluid. Thus, if an incompressible fluid is used for the study of atmospheric flows, the obtained flow pattern becomes questionable in the lower atmosphere. In particular it may happen that the incompressible flow would not display any eddies while these eddies may be present in the flow of the compressible fluid.

VII. CONCLUSIONS

Large amplitude motion in steady, two dimensional atmospheric flows past mountain ridges has been studied. For certain upstream conditions, the governing equation was exactly linear in the case of slight stratification in entropy and specific energy. These upstream conditions leave wind profile and density stratification (or the stratification of any other relevant physical quantity) quite flexible and it is possible to approximate existing atmospheric conditions rather closely.

A general criterion governing the presence of leewaves and expressed in terms of wind velocity and entropy stratification would be highly complicated. In a flow where, say, one leewave component is present, it is possible for the wave length to remain the same and this with varying stratification in entropy. This variation in stratification does not uniquely determine a change in wind profile, even if the wave length of the wave component is to be kept constant. However, roughly we can state that an increase in entropy stratification favors wave development whereas increasing the wind velocity tends to eliminate wave motion.

All the obtained flow patterns where waves in the lee are present show one or more jets extending upstream. Furthermore, they (the flow patterns) exhibit a tendency to develop downstream eddies. The presence of these eddies depends on the height of the ridge. Increasing this height may also lead to the formation of closed cells but the flow inside these cells, as calculated here, cannot be justified since the relevant streamlines do not originate far upstream.

The temperature field corresponding to a particular flow pattern (one leewave component) shows the existence of cold regions near the crests of the waves which partly explains the formation of equally spaced clouds sometimes observed in the lee of mountain ridges.

The comparison between an atmospheric flow, the air being considered compressible, and a flow of an incompressible fluid reveals clearly that, in order to approximate the flow of a compressible fluid by that of an incompressible one, the density stratification for the incompressible fluid should be taken equal to the stratification of potential density in the atmosphere. Under similar upstream conditions the flows of the compressible and incompressible fluids have then the same general characteristics. In particular, the waves present in both flows have nearly the same wave length. However, the spacing of the streamlines is more varied in the compressible flow and the wave is more developed. In particular, the amplitude of the wave in the lower atmosphere is approximately 3 times as large as the corresponding amplitude in the incompressible flow.

APPENDIX I

INTEGRATION OF EQUATION (21)

The equation is

$$\frac{d^2 \psi_1'}{dz^2} + \frac{1}{\gamma-1} \frac{\alpha}{1-\alpha z} \frac{d\psi_1'}{dz} + \beta(1-\alpha z)^{2/\gamma-1} (Az-C) \psi_1' = \beta(1-\alpha z)^{2/\gamma-1} (D-Bz). \quad (21)$$

The interval of interest to the physical problem is $0 \leq z \leq 1$. All points of this interval are ordinary points of Equation (21), provided $\alpha < 1$. It turns out that physically realistic values of α are in the neighborhood of 0.32 so that previous requirement ($\alpha < 1$) is certainly satisfied. Substitution of

$$\psi_1'(z) = \sum_{n=0}^{\infty} a_n z^n \quad (79)$$

into (21) produces, after shifting indices,

$$\begin{aligned} & \sum_{n=0}^{\infty} n(n-1)a_n z^{n-2} - \alpha \sum_{n=1}^{\infty} (n-1)(n-2)a_{n-1} z^{n-2} + \frac{\alpha}{\gamma-1} \sum_{n=1}^{\infty} (n-1)a_{n-1} z^{n-2} \\ & + A\beta \sum_{n=3}^{\infty} \left[\sum_{k=0}^{n-3} \frac{\alpha^k}{k!} \left(\frac{1+\gamma}{1-\gamma}\right)_k a_{n-k-3} \right] z^{n-2} \\ & - C\beta \sum_{n=2}^{\infty} \left[\sum_{k=0}^{n-2} \frac{\alpha^k}{k!} \left(\frac{1+\gamma}{1-\gamma}\right)_k a_{n-k-2} \right] z^{n-2} \\ & = \beta D \sum_{n=2}^{\infty} \frac{\alpha^{n-2}}{(n-2)!} \left(\frac{1+\gamma}{1-\gamma}\right)_{n-2} z^{n-2} - \beta B \sum_{n=3}^{\infty} \frac{\alpha^{n-3}}{(n-3)!} \left(\frac{1+\gamma}{1-\gamma}\right)_{n-3} z^{n-2}. \end{aligned}$$

It follows that the coefficients a_0 and a_1 are arbitrary, in agreement with the fact that the point $z = 0$ is an ordinary point of the differential equation.

The first recurrence relation is

$$a_2 = \frac{1}{2} (\beta D + \beta C a_0 - \frac{\alpha a_1}{\gamma-1}) . \quad (80)$$

For $n \geq 3$,

$$a_n = \frac{\alpha(n-2) - \frac{\alpha}{\gamma-1}}{n} a_{n-1} + \frac{\beta}{n(n-1)} \left\{ C \sum_{k=0}^{n-2} \frac{\alpha^k}{k!} \left(\frac{1+\gamma}{1-\gamma} \right)_k a_{n-k-2} \right. \\ \left. - A \sum_{k=0}^{n-3} \frac{\alpha^k}{k!} \left(\frac{1+\gamma}{1-\gamma} \right)_k a_{n-k-3} + D \frac{\alpha^{n-2}}{(n-2)!} \left(\frac{1+\gamma}{1-\gamma} \right)_{n-2} - B \frac{\alpha^{n-3}}{(n-3)!} \left(\frac{1+\gamma}{1-\gamma} \right)_{n-3} \right\} \quad (81)$$

As far as the physical problem is concerned, there is no loss in generality in requiring $\psi_1'(0) = 0$. Thus we take $a_0 = 0$. By varying a_1 , we can now get all possible stream functions corresponding to a set of values of A, B, C, and D. The value of a_1 leading to the most realistic upstream conditions should be chosen.

From a practical point of view, the selection of the most suitable stream function $\psi_1^i(z)$ is much facilitated by taking

$$\psi_1^i(z) = G \tilde{\psi}_1^i(z) + \hat{\psi}_1^i(z)$$

where $\tilde{\psi}_1^i(z)$ is a solution of the reduced equation and $\hat{\psi}_1^i(z)$ is a particular solution of the complete equation. Both solutions $\tilde{\psi}_1^i(z)$ and $\hat{\psi}_1^i(z)$ satisfy $\tilde{\psi}_1^i(0) = \hat{\psi}_1^i(0) = 0$. By varying the value of the constant G, the most suitable solution of Equation (21) can be selected.

The function $\tilde{\psi}_1^i(z)$ is represented by (79) where the coefficients are taken as follows:

$$a_0 = 0 , \\ a_1 = \text{constant} = 1 , \\ a_2 = \frac{\alpha}{2(1-\gamma)} .$$

For $n \geq 3$, the recurrence relation (81) can be used where B and D are taken equal to zero. Of course, the function $\hat{\psi}_1(z)$ is given by (79) where the coefficients a_n are to be computed from (80) and (81) taking $a_0 = 0$ and $a_1 = 0$, for example.

APPENDIX II

CALCULATION OF THE EIGENVALUES AND EIGENFUNCTIONS

The Sturm-Liouville system is

$$\frac{d^2f}{dz^2} + \frac{1}{\gamma-1} \frac{\alpha}{1-\alpha z} \frac{df}{dz} + [\beta(1-\alpha z)^{2/\gamma-1}(Az-C) + \lambda]f = 0, \quad (31)$$

$$f(0) = 0, \quad (82)$$

$$f(1) = 0. \quad (83)$$

Equation (31) has the same singular points as Equation (21) treated in Appendix I. Again we can assume a solution of the form

$$f(z) = \sum_{n=0}^{\infty} a_n z^n. \quad (84)$$

The coefficients a_n satisfy following recurrence relations:

$$a_2 = \frac{1}{2} [a_0(\beta C - \lambda) - \frac{\alpha a_1}{\gamma-1}] \quad (85)$$

and (for $n \geq 3$)

$$a_n = U_n a_{n-1} + \frac{1}{n(n-1)} \left\{ \beta C \sum_{k=0}^{n-2} V_k a_{n-k-2} - A\beta \sum_{k=0}^{n-3} V_k a_{n-k-3} + \lambda(\alpha a_{n-3} - a_{n-2}) \right\},$$

in which

$$U_n = \frac{\alpha(n-2) - \frac{\alpha}{\gamma-1}}{n} \quad (87)$$

and

$$V_k = \frac{\alpha^k}{k!} \left(\frac{1+\gamma}{1-\gamma} \right)_k. \quad (88)$$

The coefficients a_0 and a_1 are arbitrary.

Condition (82) can be satisfied simply by taking $a_0 = 0$.

The value of λ for which condition (83) is satisfied is an eigenvalue of the system and is, of course, independent of a_1 . Therefore, the coefficient a_1 can, for the time being, be set equal to 1. Its final value will be determined by the normalization process. The eigenvalues are the zeros of a function $R(\lambda)$ which will be defined as follows. A certain value of λ is assumed in Equation (31). This equation is then integrated subject to the initial conditions $f(0) = a_0 = 0$ and $df(0)/dz = a_1 = 1$. The function thus obtained is evaluated at $z = 1$ and put equal to $R(\lambda)$, i.e.,

$$R(\lambda) = f(1; \lambda),$$

Note, that for a given λ , one integration of (31) produces the corresponding value of $R(\lambda)$.

The zeros of $R(\lambda)$ can now be determined according to the following scheme. An initial value of λ is assumed, say λ_1 , and the corresponding $R(\lambda_1)$ computed; λ is then increased to λ_2 and again $R(\lambda_2)$ evaluated. If $R(\lambda_1)$ and $R(\lambda_2)$ have the same sign there is no zero of $R(\lambda)$, and hence no eigenvalue between λ_1 and λ_2 , provided the increment $\lambda_2 - \lambda_1$ has been taken small enough. The previous process (incrementing λ and calculating the corresponding R) can be repeated until a difference in sign in two successive R -values is detected. Let $R(\lambda_3)$ and $R(\lambda_2)$ have different signs. Then there must be an eigenvalue between λ_2 and λ_3 . This eigenvalue can be approximated to any degree of accuracy by successive linear interpolations. Interpolating linearly between λ_2 and λ_3 gives:

$$\lambda_4 = \frac{\lambda_2 R(\lambda_3) - \lambda_3 R(\lambda_2)}{R(\lambda_3) - R(\lambda_2)}$$

Out of the three quantities $R(\lambda_2)$, $R(\lambda_3)$ and $R(\lambda_4)$, the two having a different sign are selected, i.e., $R(\lambda_2)$ and $R(\lambda_4)$ in the case represented in Figure 19. We now know that the eigenvalue lies between λ_2 and λ_4 . A new linear interpolation gives λ_5 .

By repeating the previous procedure, the eigenvalue can be approximated as closely as desired. Once a value of λ has been accepted as an eigenvalue, the whole scheme is repeated to produce the following eigenvalue, etc.

Mathematically, the method outlined above is straightforward. However, from a practical point of view a major difficulty arises which becomes more serious as the eigenvalues grow larger and is prohibitive for only moderate values of λ . Indeed, although the convergence of the power series is guaranteed mathematically for any value of λ , the coefficients a_n behave in such a way that an accurate evaluation of $f(1)$ requires an excessive amount of significant figures in the numerical calculations. Ultimately the coefficients a_n have to decrease as n grows larger since the series $\sum_{n=1}^{\infty} a_n$ is convergent. However, before they do so, they increase up to a certain value a_N depending on λ . The larger λ , the larger a_N becomes and, as stated earlier, for only moderate λ -values the corresponding a_N becomes so large as to make the method outlined above inadequate.

The difficulty can be avoided by successively shifting the origin about which the solution is expanded. To be more exact, to evaluate $R(\lambda)$ for a given λ , the following procedure is adopted. Equation (31) is integrated as before. However, the resulting power series is only used to represent $f(z)$ in a portion of the basic interval $(0,1)$, say in the

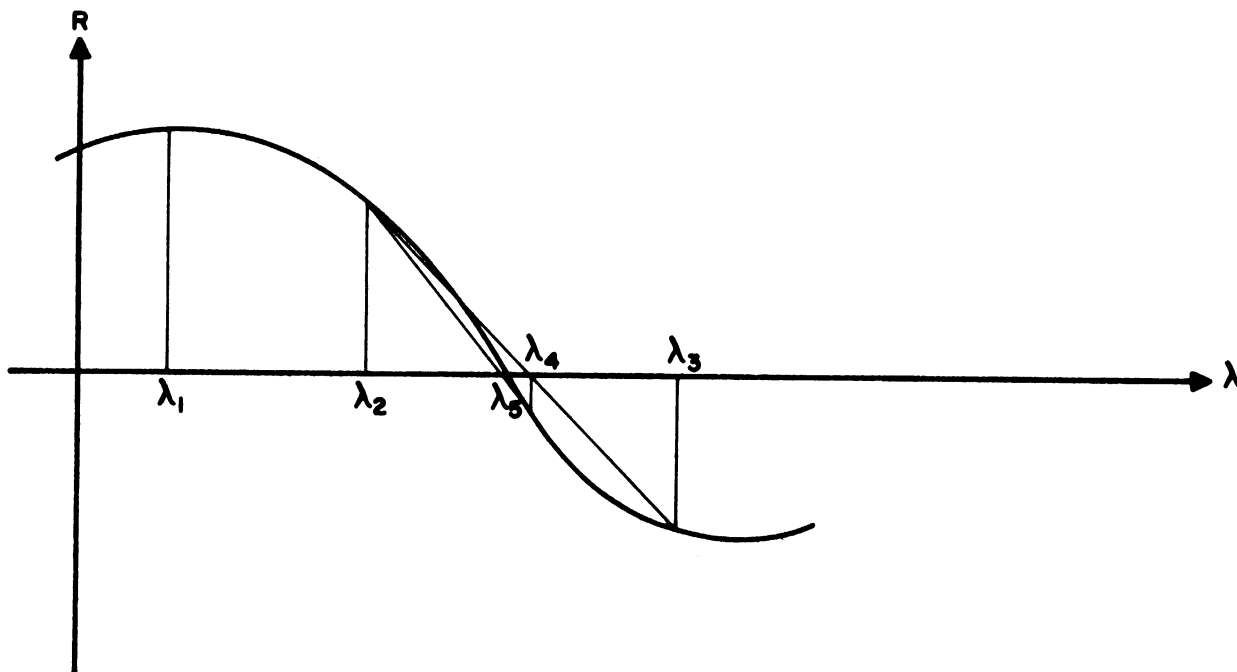


Figure 19. Iterative Scheme for the Calculation of the Eigenvalues of the Sturm-Liouville System Consisting of (31) and (32).

interval $(0, \Delta)$. The convergence at $z = \Delta$ is, of course, much faster than at $z = 1$ so that only a few terms (depending on the value of Δ) have to be taken to maintain a sufficient accuracy. What is more important, the general term remains much smaller than the previous a_n . To continue the solution analytically beyond $z = \Delta$, we shift the origin to the point $z = \Delta$, i.e., we perform the following change of independent variable

$$z' = z - \Delta .$$

The differential Equation (31) becomes

$$\frac{d^2f}{dz'^2} + \frac{1}{\gamma-1} \frac{\alpha}{p-\alpha z'} \frac{df}{dz'} + [\beta(p-\alpha z')^{2/\gamma-1}(Az'-C') + \lambda]f = 0, \quad (90)$$

in which

$$p = 1 - \alpha\Delta ,$$

$$C' = C - A\Delta .$$

Equation (90) is now integrated by assuming a solution of the form

$$f(z') = \sum_{n=0}^{\infty} b_n z'^n \quad (91)$$

subject to the initial conditions

$$[f(z')]_{z'=0} = [f(z)]_{z=\Delta} = \sum_{n=1}^{\infty} a_n \Delta^n$$

and

$$\left[\frac{df(z')}{dz'} \right]_{z'=0} = \left[\frac{df(z)}{dz} \right]_{z=\Delta} = \sum_{n=1}^{\infty} n a_n \Delta^{n-1} .$$

The coefficients b_n are given by

$$b_0 = \sum_{n=1}^{\infty} a_n \Delta^n ,$$

$$b_1 = \sum_{n=1}^{\infty} n a_n \Delta^{n-1} ,$$

$$b_2 = \frac{b_0}{2} (\beta C' p^{2/\gamma-1} - \lambda) - \frac{\alpha}{\gamma-1} \frac{b_1}{2p} ,$$

and, for $n \geq 3$,

$$b_n = \frac{U_n}{p} b_{n-1} + \frac{1}{pn(n-1)} \left\{ \beta C' \sum_{k=0}^{n-2} V_k b_{n-k-2} - A\beta \sum_{k=0}^{n-3} V_k b_{n-k-3} + \lambda(\alpha b_{n-3} - p b_{n-2}) \right\},$$

in which

$$U_n = \frac{\alpha(n-2) - \frac{\alpha}{\gamma-1}}{n}$$

and

$$V_k = \frac{\alpha^k}{k!} p^{\frac{\gamma+1}{\gamma-1} - k} \left(\frac{1+\gamma}{1-\gamma} \right)_k.$$

The power series (91) represents the analytic continuation of the function given by (84) beyond the point $z = \Delta$. It will be used to represent the solution in the interval $(\Delta, 2\Delta)$.

The previous method can be applied repeatedly to continue the solution analytically beyond the points $2\Delta, 3\Delta$, etc. Each power series represents the solution in one subinterval and the analyticity at the points $z = \Delta, 2\Delta, 3\Delta, \dots$ is established by matching the value of the function and its first derivative at these points.

If M is the number of sub-intervals and the power series $\sum_{n=0}^{\infty} q_n \xi^n$ represents the solution in the last sub-interval $[(M-1)\Delta, 1]$, the value of $R(\lambda)$ is given by $R(\lambda) = \sum_{n=0}^{\infty} q_n \Delta^n$.

APPENDIX III

CALCULATION OF THE FUNCTIONS $F_0(z)$ AND $F_1(z)$

The governing equations are

$$\frac{d^2 F_p}{dz^2} + \frac{1}{\gamma-1} \frac{\alpha}{1-\alpha z} \frac{dF_p}{dz} + [\beta(1-\alpha z)^{2/\gamma-1} (Az-C) - \frac{p^2 \pi^2}{b^2}] F_p = 0 \quad (92)$$

$$p = 0, 1$$

with the conditions

$$F_p(0) = 1, \quad (93)$$

$$F_p(1) = 0. \quad (94)$$

Let $r_p(z)$ and $s_p(z)$ be two linearly independent solutions of Equation (92) satisfying the following initial conditions

$$r_p(0) = 1, \quad \frac{dr_p(0)}{dz} = 0, \quad (95)$$

$$s_p(0) = 0, \quad \frac{ds_p(0)}{dz} = 1. \quad (96)$$

The function $F_p(z)$ can be expressed in terms of $r_p(z)$ and $s_p(z)$ as follows:

$$F_p(z) = r_p(z) - \frac{r_p(1)}{s_p(1)} s_p(z). \quad (97)$$

The solutions $r_p(z)$ and $s_p(z)$ can easily be obtained using a power series method. One can then evaluate $F_p(z)$ either by direct application of Equation (97) or by integrating Equation (92) subject to the initial conditions

$$F_p(0) = 1$$

and

$$\frac{dF_p(o)}{dz} = - \frac{r_p(1)}{s_p(1)} .$$

When using a digital computer, either method gives rise to some difficulty. This difficulty is largely due to the exponential growth of $r_1(z)$ and $s_1(z)$ in case the width is small, i.e., π/b large. Indeed, an error in $dF_p(o)/dz$, although beyond the accuracy of the computer, will cause $F_p(1)$ to be different from zero by an amount which cannot be tolerated.

The situation can again be remedied by dividing the basic interval $(0, 1)$ into a number (say 10) of sub-intervals. The adopted scheme is then the following. A solution of the form (97) is computed but only considered valid throughout the first sub-interval $(0 < z < 0.1)$. In that interval, the solution is sufficiently accurate. Indeed, although the error grows exponentially, the length of the sub-interval is chosen small enough as to make the error in $F_p(z)$ below a certain tolerable limit. The value of $F_p(z)$ and its first derivative $dF_p(z)/dz$ can now be evaluated at the end of the first sub-interval (i.e., at $z = 0.1$). If we were to continue the solution beyond $z = 0.1$, using previous values of $F_p(0.1)$ and $dF_p(0.1)/dz$, the error would be propagated and amplified in the second sub-interval. Although the error in $dF_p(0.1)/dz$ is still tolerable, it has grown to such an extent that it can be recognized by the computer and is therefore susceptible to correction. This correction can be done by re-evaluating $dF_p(0.1)/dz$ as follows: given $F_p(0.1)$, find the value of $dF_p(0.1)/dz$ that gives rise to a solution of Equation (92), vanishing at the end of the interval ($z = 1$). This problem is similar to the one already treated in this appendix and will not be repeated. The new value of $dF_p(0.1)/dz$ will

be slightly different from the former one and again, its error will be at the edge of the accuracy of the computer. The solution can now be continued into the second sub-interval ($0.1 < z < 0.2$) by the use of $F_p(0.1)$ and the corrected value of $dF_p(0.1)/dz$.

The previous process can be repeated to obtain the solution in all sub-intervals and consequently in the basic interval $(0, 1)$.

It was tacitly assumed that $(p\pi/b)^2$ is not equal to an eigenvalue of the Sturm-Liouville system consisting of (31) and (32). It would then indeed be impossible to find a solution of (92) satisfying conditions (93) and (94).

APPENDIX IV

Tables I, III, V, VII, IX, XI, XIII, XV, XVII

Eigenfunctions of the Sturm-Liouville system consisting of (31) and (32)

with $\alpha = 0.3125$, $\beta = 2.3471$, $\gamma = 1.4$.

- - -

Tables II, IV, VI, VIII, X, XII, XIV, XVI, XVIII

Numerical values of the quantities necessary for the calculation of a flow pattern according to Long's method and Yih's method ($\alpha = 0.3125$, $\beta = 2.3471$, $\gamma = 1.4$).

TABLE I
A = 0, C = 10

z	f ₁ (z)	f ₂ (z)	f ₃ (z)	f ₄ (z)	f ₅ (z)
0	0	0	0	0	0
0.05	0.1659	0.3962	0.6102	0.8029	0.9730
0.10	0.3258	0.7484	1.0805	1.2921	1.3706
0.15	0.4790	1.0302	1.3227	1.3032	0.9913
0.20	0.6237	1.2189	1.2942	0.8463	0.0737
0.25	0.7573	1.2992	1.0072	-0.1032	-0.8473
0.30	0.8764	1.2646	0.5270	-0.6468	-1.2513
0.35	0.9776	1.1190	-0.0417	-1.1272	-0.9285
0.40	1.0571	0.8770	-0.5769	-1.1696	-0.0910
0.45	1.1116	0.5629	-0.9663	-0.7746	0.7616
0.50	1.1383	0.2084	-1.1310	-0.1071	1.1390
0.55	1.1359	-0.1507	-1.0432	0.5703	0.8435
0.60	1.1009	-0.4778	-0.7315	1.0003	0.0747
0.65	1.0361	-0.7401	-0.2733	1.0296	-0.7010
0.70	0.9420	-0.9121	0.2236	0.6644	-1.0325
0.75	0.8215	-0.9784	0.6461	0.0623	-0.7472
0.80	0.6787	-0.9356	0.9020	-0.5335	-0.0407
0.85	0.5188	-0.7925	0.9406	-0.8932	0.6536
0.90	0.3478	-0.5690	0.7632	-0.8887	0.9296
0.95	0.1726	-0.2936	0.4206	-0.5397	0.6466
1.00	0	0	0	0	0

TABLE III
A = 0, C = -20

z	f ₁ (z)	f ₂ (z)	f ₃ (z)	f ₄ (z)	f ₅ (z)
0	0	0	0	0	0
0.05	0.3427	0.4772	0.6618	0.8364	0.9939
0.10	0.6466	0.8652	1.1233	1.2866	1.3322
0.15	0.8953	1.1160	1.2781	1.1836	0.8389
0.20	1.0808	1.2077	1.1074	0.6006	-0.1449
0.25	1.2020	1.1425	0.6745	-0.2012	-1.0026
0.30	1.2629	0.9426	0.0996	-0.8909	-1.2296
0.35	1.2711	0.6435	-0.4745	-1.2048	-0.7233
0.40	1.2358	0.2872	-0.9180	-1.0425	-0.1836
0.45	1.1668	-0.0833	-1.1412	-0.4919	0.9456
0.50	1.0735	-0.4295	-1.1102	0.2187	1.1323
0.55	0.9641	-0.7202	-0.8478	0.8169	0.6667
0.60	0.8459	-0.9339	-0.4233	1.0895	-0.1542
0.65	0.7244	-1.0585	0.0668	0.9558	-0.8506
0.70	0.6039	-1.0916	0.5206	0.4866	-1.0404
0.75	0.4874	-1.0383	0.8514	-0.1323	-0.6451
0.80	0.3766	-0.9106	1.0033	-0.6744	0.0857
0.85	0.2725	-0.7242	0.9591	-0.9544	0.7329
0.90	0.1754	-0.4977	0.7395	-0.8905	0.9477
0.95	0.0848	-0.2502	0.3963	-0.5248	0.6376
1.00	0	0	0	0	0

z	f ₆ (z)	f ₇ (z)	f ₈ (z)	f ₉ (z)	f ₁₀ (z)
0	0	0	0	0	0
0.02	0.5125	0.5941	0.6733	0.7496	0.8229
0.04	0.9478	1.0693	1.1736	1.2590	1.3245
0.06	1.2480	1.3398	1.3827	1.3765	1.3214
0.08	1.3743	1.3573	1.2542	1.0720	0.8224
0.10	1.3119	1.1233	0.8244	0.4450	0.0226
0.12	1.0721	0.6847	0.2018	-0.3081	-0.7729
0.14	0.6900	0.1259	-0.4597	-0.9547	-1.2650
0.16	0.2199	-0.4472	-0.9989	-1.2986	-1.2732
0.18	-0.2725	-0.9277	-1.2867	-1.2391	-0.8020
0.20	-0.7195	-1.2927	-1.2570	-0.8007	-0.0366
0.22	-1.0604	-1.2927	-0.9220	-0.1241	0.7299
0.24	-1.2500	-1.1155	-0.3681	0.5794	1.2085
0.26	-1.2643	-0.7326	0.2662	1.0931	1.2233
0.28	-1.1042	-0.2189	0.8248	1.2623	0.7762
0.30	-0.7945	0.3270	1.1727	1.0404	0.0437
0.32	-0.3802	0.8023	1.2282	0.5023	-0.6927
0.34	0.0794	1.1186	0.9826	-0.1811	-1.1547
0.36	0.5201	1.2192	0.5010	-0.7969	-1.1723
0.38	0.8810	1.0885	-0.0948	-1.1564	-0.7463
0.40	1.1131	0.7553	-0.6569	-1.1531	-0.0455
0.42	1.1864	0.2855	-1.0481	-0.7943	0.6601
0.44	1.0933	-0.2297	-1.1753	-0.1967	1.1032
0.46	0.8495	-0.6923	-1.0120	0.4508	1.1206
0.48	0.4616	-1.0158	-0.6032	0.9473	0.7132
0.50	0.0716	-1.1413	-0.0538	1.1422	0.0430
0.52	-0.3506	-1.0486	0.4988	0.9405	-0.6312
0.54	-0.7160	-0.7591	0.9185	0.5186	-1.0536
0.56	-0.9744	-0.3312	1.1045	-0.0950	-1.0686
0.58	-1.0913	0.1515	1.0153	-0.6678	-0.6780
0.60	-1.0930	0.5962	0.6778	-1.0230	-0.0375
0.62	-0.8676	0.9194	0.1798	-1.0547	0.6050
0.64	-0.5638	1.0617	-0.3528	-0.7592	1.0055
0.66	-0.1867	0.9996	-0.7083	-0.2342	1.0164
0.68	0.2093	0.7487	-1.0208	0.3531	0.6412
0.70	0.5681	0.3603	-0.9970	0.8194	0.0297
0.72	0.8397	-0.0889	-0.7277	1.0224	-0.5809
0.74	0.9875	-0.5123	-0.2842	0.9044	-0.9586
0.76	0.9931	-0.8295	0.2206	0.5082	-0.9643
0.78	0.8583	-0.9823	0.6606	-0.0377	-0.6034
0.80	0.6051	-0.9447	0.9285	-0.5606	-0.0205
0.82	0.2716	-0.7277	0.9614	-0.8988	0.5582
0.84	-0.0934	-0.3765	0.7559	-0.9510	0.9126
0.86	-0.4375	0.0392	0.3679	-0.7067	0.9125
0.88	-0.7124	0.4387	-0.1028	-0.2482	0.5652
0.90	-0.8806	0.7458	-0.5381	0.2776	0.0104
0.92	-0.9204	0.9039	-0.8309	0.7059	-0.5365
0.94	-0.8288	0.8859	-0.9118	0.9055	-0.8673
0.96	-0.6218	0.6989	-0.7652	0.8195	-0.8609
0.98	-0.3312	0.3825	-0.4324	0.4806	-0.5270
1.00	0	0	0	0	0

TABLE II
A = 0, C = 10

n	λ _n	$\frac{df_n(0)}{dz}$	$\int_0^2 \frac{1 - \cos 10\pi z}{(1-\alpha z)(1/\alpha-1)} f_n(z) dz$	$\int_0^3 \frac{1 - \cos 6.667\pi z}{(1-\alpha z)(1/\alpha-1)} f_n(z) dz$
1	28.378	3.3809	0.0709	0.1629
2	50.982	8.1767	0.1596	0.3343
3	100.41	12.858	0.2228	0.3973
4	169.51	17.423	0.2542	0.3501
5	258.34	21.937	0.2535	0.2286
6	366.90	26.427	0.2246	0.0850
7	495.21	30.903	0.1751	-0.0325
8	643.25	35.371	0.1145	-0.0964
9	811.03	39.833	0.0531	-0.1053
10	998.56	44.292	-0.0003	-0.0779

TABLE IV
A = 0, C = -20

n	λ _n	$\frac{df_n(0)}{dz}$	$\int_0^2 \frac{1 - \cos 10\pi z}{(1-\alpha z)\alpha-1} f_n(z) dz$	$\int_0^3 \frac{1 - \cos 6.667\pi z}{(1-\alpha z)(1/\alpha-1)} f_n(z) dz$
1	-12.395	7.0853	0.1382	0.2944
2	18.337	9.9957	0.1812	0.3497
3	67.285	14.152	0.2275	0.3704
4	136.19	18.419	0.2485	0.3061
5	224.93	22.745	0.2418	0.1849
6	333.44	27.105	0.2102	0.0519
7	461.71	31.487	0.1604	-0.0515
8	609.73	35.884	0.1013	-0.1029
9	777.50	40.290	0.0426	-0.1819
10	965.01	44.703	-0.0078	-0.2732

TABLE V
A = 0, C = -50

x	f ₁ (x)	f ₂ (x)	f ₃ (x)	f ₄ (x)	f ₅ (x)
0	0	0	0	0	0
0.05	0.5303	0.5319	0.6956	0.8609	1.0097
0.10	0.9692	0.9222	1.1280	1.2624	1.2842
0.15	1.2792	1.1037	1.1798	1.0443	0.6825
0.20	1.4525	1.0662	0.8697	0.3523	-0.3455
0.25	1.5029	0.8436	0.3208	-0.4702	-1.1131
0.30	1.4560	0.4959	-0.2941	-1.0591	-1.1544
0.35	1.3412	0.0911	-0.8090	-1.1859	-0.4881
0.40	1.1863	-0.3091	-1.1067	-0.8326	0.4431
0.45	1.0144	-0.6750	-1.1380	-0.1713	1.0763
0.50	0.8426	-0.9226	-0.9209	0.5264	1.0650
0.55	0.6823	-1.0924	-0.5237	1.0020	0.4545
0.60	0.5397	-1.1669	-0.0420	1.1020	-0.3802
0.65	0.4175	-1.1559	0.4256	0.8182	-0.9705
0.70	0.3158	-1.0744	0.7967	0.2733	-1.0147
0.75	0.2327	-0.9412	1.0168	-0.3350	-0.5226
0.80	0.1658	-0.7723	1.0641	-0.8070	-0.2168
0.85	0.1120	-0.5831	0.9469	-1.0039	0.8086
0.90	0.0684	-0.3858	0.6979	-0.8844	0.9617
0.95	0.0320	-0.1894	0.3644	-0.5065	0.6267
1.00	0	0	0	0	0

TABLE VII
A = 10, C = 10

x	f ₁ (x)	f ₂ (x)	f ₃ (x)	f ₄ (x)	f ₅ (x)
0	0	0	0	0	0
0.05	0.1594	0.3870	0.6039	0.7988	0.9704
0.10	0.3143	0.7339	1.0734	1.2907	1.3730
0.15	0.4647	1.0154	1.3214	1.3107	1.0032
0.20	0.6090	1.2084	1.3026	0.8641	0.0911
0.25	0.7442	1.2960	1.0253	0.1250	-0.8341
0.30	0.8665	1.2694	0.5512	-0.6285	-1.2496
0.35	0.9716	1.1308	-0.0169	-1.1184	-0.9380
0.40	1.0552	0.8933	-0.5568	-1.1717	-0.1046
0.45	1.1133	0.5806	-0.9537	-0.7842	0.7520
0.50	1.1427	0.2246	-1.1264	-0.1187	1.1371
0.55	1.1410	-0.1379	-1.0447	0.5615	0.8475
0.60	1.1073	-0.4693	-0.7360	0.9962	0.0801
0.65	1.0418	-0.7357	-0.2781	1.0294	-0.6976
0.70	0.9464	-0.9108	0.2202	0.6658	-1.0316
0.75	0.8243	-0.9788	0.6444	0.0636	-0.7475
0.80	0.6800	-0.9366	0.9014	-0.5330	-0.0409
0.85	0.5189	-0.7933	0.9405	-0.8931	0.6537
0.90	0.3475	-0.5693	0.7629	-0.8885	0.9296
0.95	0.1722	-0.2937	0.4204	-0.5395	0.6465
1.00	0	0	0	0	0

x	f ₆ (x)	f ₇ (x)	f ₈ (x)	f ₉ (x)	f ₁₀ (x)
0	0	0	0	0	0
0.02	0.5351	0.6129	0.6889	0.7627	0.8338
0.04	0.9753	1.0869	1.1829	1.2613	1.3208
0.06	1.2519	1.3253	1.3541	1.3366	1.2728
0.08	1.3246	1.2834	1.1638	0.9720	0.7189
0.10	1.1868	0.9761	0.6696	0.2953	-0.1115
0.12	0.8651	0.4784	0.0074	-0.4669	-0.8847
0.14	0.4139	-0.1201	-0.6462	-1.0655	-1.2968
0.16	-0.0940	-0.6786	-1.1213	-1.3100	-1.1924
0.18	-0.5793	-1.0907	-1.2984	-1.1285	-0.6222
0.20	-0.9686	-1.2765	-1.1380	-0.5877	0.1819
0.22	-1.2054	-1.2036	-0.6881	0.1323	0.9020
0.24	-1.2577	-0.8923	-0.0697	0.7983	1.2596
0.26	-1.1280	-0.4093	0.5562	1.1995	1.2288
0.28	-0.8288	0.1463	1.0306	1.2140	0.5542
0.30	-0.4079	0.6638	1.2368	0.8448	-0.2187
0.32	0.0594	1.0431	1.1284	0.2159	-0.8944
0.34	0.4798	1.2134	0.7390	-0.4701	-1.2152
0.36	0.8798	1.1462	0.1718	-0.9972	-1.0651
0.38	1.1172	0.8598	-0.4283	-1.2038	-0.5107
0.40	1.1918	0.4138	-0.9118	-1.0322	0.2288
0.42	1.0967	-0.1033	-1.1615	-0.5431	0.8682
0.44	0.8493	-0.5917	-1.1207	0.1054	1.1668
0.46	0.4878	-0.9595	-0.8056	0.7099	1.0181
0.48	0.0650	-1.1401	-0.2989	1.0848	0.4872
0.50	-0.3591	-1.1038	0.2714	1.1196	-0.2179
0.52	-0.7261	-0.8620	0.7654	0.8105	-0.8281
0.54	-0.9872	-0.4643	1.0647	0.2592	-1.1159
0.56	-1.1094	0.0120	1.1010	-0.3611	-0.9796
0.58	-1.0792	0.4773	0.8711	-0.8598	-0.4791
0.60	-0.9044	0.8460	0.4361	-1.0879	0.1912
0.62	-0.6118	1.0526	-0.0953	-0.9818	0.7774
0.64	-0.2432	1.0630	-0.5937	-0.5806	1.0627
0.66	0.1506	0.8795	-0.9409	-0.0118	0.9473
0.68	0.5168	0.5400	-1.0574	0.5495	0.4822
0.70	0.8079	0.1094	-0.9205	0.9345	-0.1526
0.72	0.9874	-0.3325	-0.5682	1.0313	-0.7184
0.74	1.0345	-0.7058	-0.0885	0.8170	-1.0073
0.76	0.9462	-0.9449	0.4024	0.3625	-0.9184
0.78	0.7372	-1.0103	0.7886	-0.1912	-0.4926
0.80	0.4374	-0.8941	0.9818	-0.6765	0.1059
0.82	0.0875	-0.6212	0.9408	-0.9504	0.6532
0.84	-0.2664	-0.2437	0.6805	-0.9360	0.9492
0.86	-0.5788	0.1691	0.2668	-0.6440	0.8907
0.88	-0.8111	0.5433	-0.2005	-0.1671	0.5070
0.90	-0.9356	0.8138	-0.6111	0.3490	-0.0541
0.92	-0.9391	0.9354	-0.8710	0.7509	-0.5834
0.94	-0.8243	0.8904	-0.9233	0.9224	-0.8882
0.96	-0.6084	0.6905	-0.7606	0.8181	-0.8622
0.98	-0.3211	0.3744	-0.4257	0.4751	-0.5225
1.00	0	0	0	0	0

TABLE VI
A = 0, C = -50

n	λ _n	$\frac{df_n(0)}{dx}$	$\int_0^2 \frac{1-\cos 10\pi x}{1-x^2} f_n(x) dx$	$\int_0^3 \frac{1-\cos 6.667\pi x}{(1-x)(1/x^2-1)} f_n(x) dx$
1	-52.118	11.094	0.2044	0.4106
2	-12.582	11.315	0.1893	0.3327
3	35.457	15.102	0.2241	0.3288
4	103.67	19.249	0.2392	0.2589
5	192.05	23.461	0.2286	0.1427
6	300.36	27.729	0.1953	0.0217
7	428.50	32.036	0.1458	-0.0678
8	576.44	36.372	0.0886	-0.1077
9	744.15	40.729	0.0325	-0.1014
10	931.62	45.102	-0.0148	-0.0683

TABLE VIII
A = 10, C = 10

n	λ _n	$\frac{df_n(0)}{dx}$	$\int_0^2 \frac{1-\cos 10\pi x}{(1-x)^{1/2}} f_n(x) dx$	$\int_0^3 \frac{1-\cos 6.667\pi x}{(1-x)(1/x^2-1)} f_n(x) dx$
1	15.693	3.2418	0.0685	0.1585
2	46.804	7.9760	0.1567	0.3302
3	96.357	12.707	0.2217	0.3977
4	165.49	17.309	0.2542	0.3529
5	254.33	21.846	0.2543	0.2320
6	362.90	26.352	0.2258	0.0879
7	491.21	30.839	0.1763	-0.0306
8	639.26	35.315	0.1157	-0.0955
9	807.04	39.783	0.0541	-0.1052
10	994.57	44.247	0.0004	-0.0781

TABLE XIII

A = 20, C = 10

x	f ₁ (x)	f ₂ (x)	f ₃ (x)	f ₄ (x)	f ₅ (x)
0	0	0	0	0	0
0.05	2.1532	0.3780	0.5975	0.7957	0.9678
0.10	0.3034	0.7195	1.0661	1.2891	1.3753
0.15	0.4512	1.0004	1.3196	1.3180	1.0150
0.20	0.5950	1.1976	1.5104	0.8813	0.1085
0.25	0.7317	1.2922	1.0429	0.1467	-0.8207
0.30	0.8569	1.2736	0.5750	-0.6100	-1.2477
0.35	0.9658	1.1419	0.0077	-1.1094	-0.9473
0.40	1.0534	0.9089	-0.5366	-1.1736	-0.1181
0.45	1.1150	0.5976	-0.9411	-0.7937	0.7423
0.50	1.1469	0.2403	-1.1217	-0.1302	1.1551
0.55	1.1467	-0.1256	-1.0460	0.5527	0.8515
0.60	1.1133	-0.4612	-0.7405	0.9921	0.0856
0.65	1.0472	-0.7316	-0.2289	1.0291	-0.6941
0.70	0.9505	-0.9037	0.2167	-1.0507	-0.7479
0.75	0.8268	-0.9795	0.6426	0.0649	-0.0412
0.80	0.6810	-0.9378	0.9009	-0.5325	0.6537
0.85	0.5189	-0.7942	0.9403	-0.8930	0.9296
0.90	0.3469	-0.5698	0.7627	-0.8884	0.6463
0.95	0.1718	-0.2938	0.4201	-0.5393	0
1.00	0	0	0	0	0

TABLE XV

A = 20, C = -20

z	f ₁ (z)	f ₂ (z)	f ₃ (z)	f ₄ (z)	f ₅ (z)
0	0	0	0	0	0
0.05	0.3162	0.4654	0.6526	0.8295	0.9897
0.10	0.6015	0.8504	1.1163	1.2874	1.3388
0.15	0.8423	1.1091	1.2859	1.2031	0.8638
0.20	1.0302	1.2169	1.1355	0.6371	-0.1123
0.25	1.1615	1.1707	0.7191	-0.1606	-0.9821
0.30	1.2372	0.9875	0.1503	-0.8623	-1.2332
0.35	1.2614	0.6988	-0.4296	-1.1978	-0.7465
0.40	1.2408	0.3453	-0.8876	-1.0557	0.1569
0.45	1.1836	-0.0295	-1.1283	-0.5160	0.9303
0.50	1.0982	-0.3849	-1.1122	0.1954	1.1328
0.55	0.9930	-0.6872	-0.8589	0.8020	0.6772
0.60	0.8756	-0.9120	-0.4369	1.0846	-0.1431
0.65	0.7522	-1.0457	0.0553	0.9575	-0.8446
0.70	0.6281	-1.0849	0.5132	0.4902	-1.0394
0.75	0.5070	-1.0551	0.8478	-0.1299	-0.6460
0.80	0.3914	-0.9086	1.0019	-0.6736	0.0854
0.85	0.2829	-0.7226	0.9582	-0.9543	0.7332
0.90	0.1817	-0.4962	0.7385	-0.8902	0.9477
0.95	0.0878	-0.2492	0.3955	-0.5243	0.6372
1.00	0	0	0	0	0

x	f ₆ (x)	f ₇ (x)	f ₈ (x)	f ₉ (x)	f ₁₀ (x)
0	0	0	0	0	0
0.02	0.5098	0.5919	0.6714	0.7481	0.8216
0.04	0.9442	1.0670	1.1722	1.2585	1.3246
0.06	1.2462	1.3398	1.3848	1.3800	1.3258
0.08	1.3772	1.3632	1.2622	1.0812	0.8322
0.10	1.3215	1.1360	0.8384	0.4589	0.0353
0.12	1.0891	0.7034	0.2196	-0.2930	-0.7619
0.14	0.7133	0.1480	-0.4421	-0.9434	-1.2607
0.16	0.2471	-0.4257	-0.9852	-1.2955	-1.2784
0.18	-0.2451	-0.9111	-1.2227	-0.8157	-0.2602
0.20	-0.6958	-1.2132	-1.2634	-0.8162	-0.0539
0.22	-1.0438	-1.2951	-0.9376	-0.1435	0.7155
0.24	-1.2429	-1.1280	-0.3892	0.5619	1.2025
0.26	-1.2679	-0.7529	0.2447	1.0830	1.2280
0.28	-1.1177	-0.2432	0.8022	1.2625	0.7897
0.30	-0.8157	0.3035	1.1648	1.0506	0.0607
0.32	-0.4060	0.7838	1.2305	0.5189	-0.6788
0.34	0.0530	1.1085	0.9940	-0.1635	-1.1488
0.36	0.4966	1.2184	0.5181	-0.7836	-1.1760
0.38	0.8633	1.0966	-0.0765	-1.1511	-0.7575
0.40	1.1102	0.7699	-0.6419	-1.1566	-0.0593
0.42	1.1848	0.3033	-1.0396	-0.8046	0.6489
0.44	1.0992	-0.2125	-1.1746	-0.2101	1.0984
0.46	0.8612	-0.6784	-1.0182	0.4387	1.1232
0.48	0.5067	-1.0075	-0.6140	0.9400	0.7212
0.50	0.0876	-1.1392	-0.0659	1.1410	0.0528
0.52	-0.3361	-1.0522	0.4883	0.9848	-0.6234
0.54	-0.7047	-0.7667	0.9119	0.5262	-1.0502
0.56	-0.9672	-0.3407	1.1026	-0.0869	-1.0700
0.58	-1.0883	0.1422	1.0176	-0.6616	-0.6827
0.60	-1.0539	0.5888	0.6829	-1.0201	-0.0432
0.62	-0.8713	0.9147	0.1859	-1.0552	0.6005
0.64	-0.5691	1.0600	-0.3475	-0.7621	1.0035
0.66	-0.1924	1.0004	-0.7847	-0.2381	1.0170
0.68	0.2042	0.7510	-1.0193	0.3497	0.6433
0.70	0.5641	0.3633	-0.9973	0.8173	0.0322
0.72	0.8371	-0.0861	-0.7290	1.0218	-0.5791
0.74	0.9861	-0.5101	-0.2858	0.9047	-0.9578
0.76	0.9925	-0.8282	0.2192	0.5090	-0.9644
0.78	0.8582	-0.9816	0.6597	-0.0369	-0.6038
0.80	0.6051	-0.9444	0.9280	-0.5601	-0.0208
0.82	0.2715	-0.7275	0.9611	-0.8985	0.5581
0.84	-0.0936	-0.3762	0.7557	-0.9507	0.9125
0.86	-0.4379	0.0397	0.3673	-0.7064	0.9123
0.88	-0.7128	0.4391	-0.1033	-0.2477	0.5649
0.90	-0.8808	0.7462	-0.5386	0.2781	0.0099
0.92	-0.9204	0.9041	-0.8512	0.7061	-0.5369
0.94	-0.8287	0.8858	-0.9118	0.9051	-0.8675
0.96	-0.6216	0.6988	-0.7651	0.8194	-0.8609
0.98	-0.3310	0.3824	-0.4323	0.4806	-0.5270
1.00	0	0	0	0	0

TABLE XIV

A = 20, C = 10

n	λ _n	$\frac{df_n(0)}{dx}$	$\int_0^2 \frac{1-\cos 10nx}{(1-\cos x)^{1/2}-1} f_n(x) dx$	$\int_0^3 \frac{1-\cos 6.667nx}{(1-\cos x)^{1/2}-1} f_n(x) dx$
1	11.000	3.1103	0.0663	0.1544
2	42.616	7.7778	0.1539	0.3261
3	92.306	12.554	0.2205	0.3980
4	161.47	17.193	0.2543	0.3557
5	250.33	21.754	0.2551	0.2354
6	358.91	26.275	0.2270	0.0908
7	487.22	30.774	0.1776	-0.0288
8	635.27	35.258	0.1169	-0.0947
9	803.05	39.733	0.0551	-0.1051
10	990.58	44.201	0.0012	-0.0784

TABLE XVI

A = 20, C = -20

n	λ _n	$\frac{df_n(0)}{dx}$	$\int_0^2 \frac{1-\cos 10nx}{(1-\cos x)^{1/2}-1} f_n(x) dx$	$\int_0^3 \frac{1-\cos 6.667nx}{(1-\cos x)^{1/2}-1} f_n(x) dx$
1	-21.290	6.5155	0.1290	0.2784
2	9.9346	9.7175	0.1786	0.3491
3	59.104	13.912	0.2267	0.3743
4	128.09	18.222	0.2493	0.3126
5	216.87	22.580	0.2437	0.1916
6	325.41	26.965	0.2126	0.0572
7	453.70	31.365	0.1629	-0.0482
8	601.73	35.776	0.1037	-0.1016
9	769.50	40.193	0.0445	-0.1038
10	957.02	44.616	-0.0064	-0.0738

TABLE XVII

A = 20, C = -50

z	$f_1(z)$	$f_2(z)$	$f_3(z)$	$f_4(z)$	$f_5(z)$
0	0	0	0	0	0
0.05	0.4989	0.5259	0.6892	0.8560	-1.0064
0.10	0.9187	0.9195	1.1270	1.2662	1.2923
0.15	1.2251	1.1148	1.1954	1.0665	0.7079
0.20	1.4081	1.0966	0.9042	0.3886	-0.3158
0.25	1.4761	0.8923	0.3669	-0.4349	-1.0987
0.30	1.4491	0.5563	-0.2487	-1.0399	-1.1644
0.35	1.3523	0.1542	-0.7756	-1.1891	-0.5142
0.40	1.2110	-0.2515	-1.0912	-0.8532	0.4183
0.45	1.0475	-0.6107	-1.1398	-0.1977	1.0657
0.50	0.8791	-0.8901	-0.9345	0.5049	1.0698
0.55	0.7182	-1.0731	-0.5420	0.9909	0.4668
0.60	0.5724	-1.1581	-0.0589	1.1005	-0.3695
0.65	0.4455	-1.1542	0.4134	0.8218	-0.9657
0.70	0.3384	-1.0768	0.7897	0.2775	-1.0144
0.75	0.2502	-0.9442	1.0135	-0.3327	-0.5236
0.80	0.1785	-0.7747	1.0625	-0.8064	0.2166
0.85	0.1207	-0.5844	0.9457	-1.0038	0.8090
0.90	0.0736	-0.3862	0.6966	-0.8839	0.9618
0.95	0.0344	-0.1894	0.3635	-0.5059	0.6264
1.00	0	0	0	0	0

z	$f_6(z)$	$f_7(z)$	$f_8(z)$	$f_9(z)$	$f_{10}(z)$
0	0	0	0	0	0
0.02	0.5329	0.6110	0.6873	0.7614	0.8327
0.04	0.9726	1.0851	1.1819	1.2611	1.3211
0.06	1.2516	1.3266	1.3569	1.3404	1.2775
0.08	1.3294	1.2903	1.1723	0.9814	0.7286
0.10	1.1982	0.9894	0.6835	0.3088	-0.0994
0.12	0.8831	-0.4908	-0.0242	-0.4532	-0.8752
0.14	0.4368	-0.0998	-0.6310	-1.0566	-1.2946
0.16	-0.0693	-0.6606	-1.1122	-1.3698	-1.1996
0.18	-0.5566	-1.0792	-1.2986	-1.1380	-0.6368
0.20	-0.9518	-1.2744	-1.1481	-0.6044	0.1653
0.22	-1.1974	-1.2118	-0.7060	0.1136	0.8899
0.24	-1.2598	-0.9093	-0.0908	0.7835	1.2569
0.26	-1.1341	-0.4318	0.5372	1.1935	1.1306
0.28	-0.8429	0.1228	1.0185	1.2185	0.5692
0.30	-0.4329	0.6440	1.2344	0.8581	-0.2023
0.32	0.0334	1.0306	1.1359	0.2334	-0.8830
0.34	0.4868	1.2101	0.7540	-0.4539	-1.2127
0.36	0.8623	1.1522	0.1901	-0.9872	-1.0719
0.38	1.1075	0.8732	-0.4114	-1.2026	-0.5235
0.40	1.1905	0.4314	-0.9002	-1.0392	0.2153
0.42	1.1032	-0.0852	-1.1575	-0.5555	0.8590
0.44	0.8618	-0.5764	-1.1243	0.0920	1.1648
0.46	0.5038	-0.9495	-0.8150	0.6995	1.0230
0.48	0.0819	-1.1365	-0.3112	1.0801	0.4964
0.50	-0.3437	-1.1063	0.2596	1.1211	-0.2083
0.52	-0.7141	-0.8692	0.7567	0.8168	-0.8217
0.54	-0.9796	-0.4741	1.0606	0.2676	-1.1143
0.56	-1.1063	0.0019	1.1016	-0.3533	-0.9826
0.58	-1.0802	0.4687	0.8753	-0.8548	-0.4846
0.60	-0.9084	0.8401	0.4422	-1.0864	0.1855
0.62	-0.6175	1.0498	-0.0891	-0.9835	0.7736
0.64	-0.2494	1.0630	-0.5889	-0.5842	1.0616
0.66	0.1448	0.8816	-0.9382	-0.0158	0.9485
0.68	0.5122	0.5431	-1.0457	0.5464	0.4846
0.70	0.8047	0.1125	-0.9213	0.9329	-0.1502
0.72	0.9856	-0.3299	-0.5697	1.0310	-0.7168
0.74	1.0337	-0.7040	-0.0902	0.8176	-1.0067
0.76	0.9460	-0.9439	0.4011	0.3633	-0.9186
0.78	0.7372	-1.0098	0.7879	-0.1905	-0.4930
0.80	0.4373	-0.8938	0.9814	-0.6761	0.1056
0.82	0.0872	-0.6209	0.9405	-0.9502	0.6531
0.84	-0.2668	-0.2432	0.6801	-0.9358	0.9491
0.86	-0.5794	0.1697	0.2662	-0.6436	0.8905
0.88	-0.8116	0.5439	-0.2011	-0.1666	0.5066
0.90	-0.9359	0.8142	-0.6116	0.3496	-0.0546
0.92	-0.9392	0.9356	-0.8713	0.7513	-0.5859
0.94	-0.8242	0.8904	-0.9233	0.9225	-0.8884
0.96	-0.6082	0.6903	-0.7605	0.8180	-0.8622
0.98	-0.3209	0.3742	-0.4256	0.4750	-0.5224
1.00	0	0	0	0	0

TABLE XVIII

A = 20, C = -50

n	λ_n	$\frac{df_n(0)}{dz}$	$\int_0^2 \frac{1-\cos 10\pi z}{(1-\alpha z)^{1/\gamma-1}} f_n(z) dz$	$\int_0^3 \frac{1-\cos 6.667\pi z}{(1-\alpha z)^{1/\gamma-1}} f_n(z) dz$
1	-60.300	10.406	0.1943	0.3949
2	-21.239	11.152	0.1894	0.3378
3	27.176	14.919	0.2245	0.3348
4	95.515	19.080	0.2406	0.2659
5	183.95	23.313	0.2307	0.1492
6	292.29	27.598	0.1978	0.0266
7	420.46	31.920	0.1483	-0.0650
8	568.41	36.268	0.0908	-0.1066
9	736.13	40.636	0.0343	-0.1016
10	923.61	45.017	-0.0135	-0.0689

BIBLIOGRAPHY

1. Crapper, G. D. "A Three-Dimensional Solution for Waves in the Lee of Mountains." Journal of Fluid Mechanics, 6, (1959) 51-76.
2. Ince, E. L. Ordinary Differential Equations. Dover Publications Inc.
3. Long, R. R. "Some Aspects of the Flow of Stratified Fluids. I - A Theoretical Investigation." Tellus, 5, (1953) 42-47.
4. Long, R. R. "Some Aspects of the Flow of Stratified Fluids. III - Continuous Density Gradients." Tellus, 7, (1955) 342-57.
5. Lyra, G. "Theorie der stationären Leewellenströmung in freier Atmosphäre." Z. angew. Math. u. Mech., Berlin, 23, (1943) 1-28.
6. Queney, P. Theory of Perturbations in Stratified Currents with Applications to Air Flow Over Mountain Barriers. Misc. Rep. No. 23, Dept. Met., University of Chicago, 1947.
7. Queney, P. "The Problem of Air Flow Over Mountains: A Summary of Theoretical Results." Bull. Amer. Met. Soc., 29, (1948) 16-25.
8. Rainville, E. D. Intermediate Course in Differential Equations. New York: John Wiley and Sons, Inc., London: Chapman and Hall, Ltd.
9. Scorer, R. S. "Theory of Waves in the Lee of Mountains." Quart. J.R. Met. Soc., 75, (1949) 41-56.
10. Scorer, R. S. "Theory of Airflow Over Mountains: II - The Flow Over A Ridge." Quart. J. R. Met. Soc., 79, (1953) 70-83.
11. Scorer, R. S. "Theory of Airflow Over Mountains: III - Airstream Characteristics." Quart. J. R. Met. Soc., 80, (1954) 417-28.
12. Scorer, R. S. and Wilkinson, M. "Waves in the Lee of an Isolated Hill." Quart. J. R. Met. Soc., 82, (1956) 419-27.
13. Yih, C. S. "A Transformation for Non-Homentropic Flows With an Application to Large-Amplitude Motion in the Atmosphere." J. Fluid Mech., 9, Part 1, (1960) 68-90.
14. Yih, C. S. "Exact Solutions for Steady Two-Dimensional Flow of a Stratified Fluid." J. Fluid Mech., 9, Part 2, (1960) 161-74.

UNIVERSITY OF MICHIGAN



3 9015 02828 4076